chemengineering

MDPI

Review

Solar Fuels by Heterogeneous Photocatalysis: From Understanding Chemical Bases to Process Development

Alberto Olivo, Danny Zanardo, Elena Ghedini, Federica Menegazzo and Michela Signoretto *

CatMat Lab, Department of Molecular Sciences and Nanosystems, Ca' Foscari University Venice and Consortium INSTM, RU of Venice, Via Torino 155, 30172 Venezia, Italy; alberto.olivo@unive.it (A.O.); danny.zanardo@unive.it (D.Z.); gelena@unive.it (E.G.); fmenegaz@unive.it (F.M.)

* Correspondence: miky@unive.it; Tel.: +39-041-234-8650

Received: 30 July 2018; Accepted: 30 August 2018; Published: 4 September 2018

Abstract: The development of sustainable yet efficient technologies to store solar light into high energy molecules, such as hydrocarbons and hydrogen, is a pivotal challenge in 21st century society. In the field of photocatalysis, a wide variety of chemical routes can be pursued to obtain solar fuels but the two most promising are carbon dioxide photoreduction and photoreforming of biomass-derived substrates. Despite their great potentialities, these technologies still need to be improved to represent a reliable alternative to traditional fuels, in terms of both catalyst design and photoreactor engineering. This review highlights the chemical fundamentals of different photocatalytic reactions for solar fuels production and provides a mechanistic insight on proposed reaction pathways. Also, possible cutting-edge strategies to obtain solar fuels are reported, focusing on how the chemical bases of the investigated reaction affect experimental choices.

Keywords: solar fuels; photocatalysis; carbon dioxide photoreduction; photoreforming; process design

1. Why Do We Need Renewable Energy? Prospects and Challenges in Solar Fuels Production

Modern society is intrinsically dependent on reliable and efficient energy sources to sustain its activities. Since the beginning of the industrial revolution at the end of eighteenth century, fossil fuels by combustion have proved to be more consistent energy sources than biomass [1,2].

Among the scientific community there is still a debate on how long fossil fuels will be available, due to the intrinsic uncertainty of reserve estimations [3]. According to Shafiee and Topal in 2009, oil, coal and gas reservoirs will be finished in 35, 107 and 37 years respectively [4]. In recent years this value has not decreased much: in fact, fossil fuel utilisation has been accompanied by technological improvements in the exploitation of shale gas, shale oil, tar sands and hydrocarbon hydrates [5,6]. Despite this, the durability of fossil fuels is a significant concern, and the most critical issue is their intrinsic unsustainability. Fossil fuels do not satisfy the definition of sustainability provided by the World Commission on Environment and Development [7] since their utilisation rate is much higher than their formation, reducing their availability for future generations. However, their worldwide distribution network, efficiency, and most importantly, lower cost (27 €/MWh for coal and 39 €/MWh for natural gas [8]) compared to alternative energy sources (75 €/MWh for biomass [8]) encourages their continued utilisation.

On the contrary, the cost of fossil fuel combustion on the environment is extremely high. Due to the presence of nitrogen and sulphur impurities, and in the case of coal, metal traces, fossil fuel combustion for heating and electricity generation yields products other than water and carbon dioxide (CO_2), such as methane (CH_4), nitrogen oxides (NO_x) and sulphur oxides (SO_x), as well as particulate matter (PM), with detrimental effects for both humans and the environment [9,10]. Most importantly,

fossil fuels represent the main cause of CO_2 emissions in the atmosphere: their global related CO_2 emissions grew approximately 25% in the period between 1990 and 2004 [11] and in December 2017, CO_2 concentration reached 408 ppm, the highest observed value in human history. This value will grow to by 2.8 ppm/year in the foreseeable future [12].

Increasing CO_2 emissions represent the most important threat to the atmosphere and environment since it has been established that there is a clear connection between anomalous global warming and CO_2 emissions [13,14]. Due to the anthropogenic origin of these huge environmental phenomena, the word Anthropocene was coined to describe this particular historical moment we are living in. According to Crutzen, the Anthropocene started in the 1960s, when the effects of human activities on climate and environment became relevant [15]. In the late 1990s, policymakers' search for solid solutions to the environmental threat of CO_2 led to the Kyoto Protocol of 1997 [16] and their efforts were recently renewed by the Paris Agreement in December 2015, a treaty endorsed by 194 countries aimed at keeping world average temperature increase below 2 °C [17]. There are several strategies to pursue this aim [18]:

- to increase efficiency in energy production and consumption processes;
- to improve the ability to capture and sequester CO_2 from the atmosphere and its utilisation;
- to decrease the carbon intensity of the economic system.

While the first strategy relies on optimising already existing technologies for the production and utilisation of traditional fuels, the other two rely on finding either new strategies to obtain alternative energy products or new energy sources. In other words, they require the replacement of fossil fuels, which the world depends on for 80% of energy production [19]. This would mean a complete change in the paradigm of energy and transportation technologies, and thus a transition from Anthropocene to Sustainocene, an era in which economic and social wealth meets wise and responsible use of environmental resources [20]. Considering these last two strategies more closely, one of them relies on CO_2 as an alternative and sustainable source for the same C-based molecules already used as fuels. Such an approach to CO_2 utilisation could be a significant opportunity for innovative industrial processes and also fit Circular Economy dictamens, providing a concrete integration of economic activities and social and environmental wellbeing in a sustainable way [21].

Conversely, reduction of carbon intensity in the economy represents a more radical approach, which pursues the use of alternative C-free energy vectors and intrinsically unties energy production from carbon dioxide emissions. Nowadays, several C-free energy technologies are available (such as hydropower, geothermal, wind, nuclear, ocean energy and photovoltaics [22]), however, they suffer from being efficient for electricity only, limiting their application in the automotive industry. Recently, among the alternative non-hydrocarbon fuels, hydrogen is an emerging fuel for the future for several reasons: no harmful combustion products are produced; it can be obtained through several technologies and from several sources, and its high diffusivity and high heat capacity make hydrogen generally safer than other fuels [23,24]. Moreover, it can be directly used in highly efficient devices, i.e., fuel cells [25–27].

Nonetheless, several issues make hydrogen uncompetitive with traditional fuels such as hydrocarbons: insufficient supply for a worldwide market, severe and energy demanding production processes, and last but not least, lack of transportation networks and fuel cells' cost [25,28]. Due to the issues related to direct utilisation of hydrogen as a fuel, it can be used indirectly to produce new attractive fuels from different sources, especially those that are bio-derived [29–32]. Nowadays hydrogen is produced mainly from fossil fuels which account for 96% of its production capacity [33,34], but an appealing method to couple sustainable hydrogen production and renewable biomass valorisation is oxygenate compounds reforming [35–38], which can be used as a hydrogen-storage medium converting into hydrogen on-board through reforming processes, then fed into a fuel cell [39].

This kind of energy source is readily available: Sims et al. assessed that 100 EJ/year of raw lignocellulose could be available worldwide at 2–3 $/GJ [40], while Long et al. estimated 251–1272 EJ/year of biomass from surplus cultivated land [41].

As reviewed by Li et al., several sources and technologies are available to produce bio-derived hydrogen [42]. Steam-reforming requires high temperatures (300–800 °C) [43,44], aqueous phase reforming can reduce operative temperatures (220–270 °C) but requires high pressure (25–30 MPa) while plasma reforming, despite its efficiency, requires electric energy [45]. Photocatalytic reforming, known as photoreforming (PR), has the advantages of mild operational conditions [46] and exploits solar light, the most abundant and widespread renewable energy [47].

Both CO_2 reduction and hydrogen formation are uphill processes, since the products' energy is higher compared to reagents. In fact, if we consider Gibbs free energy of formation for most simple compounds, CO_2 and water are characterised by the lowest value of all C-based molecules (-394.0 and -228.4 kJ·mol^{-1}), indicating that any transformation requires energy [48].

Required energy to perform this reaction can be provided in different ways, generally either as heat or electricity. Promising results were obtained both in CO_2 reduction by methanation and in steam reforming of biomass-derived alcohols [49–51]; however, these processes require temperatures higher than 400 °C, increasing the final cost of the alternative fuel [52–55].

A promising alternative energy source is sunlight. The big advantage of sunlight exploitation is that it is available almost anywhere on the Earth's surface, it can be considered renewable on a human time scale. and most importantly, it is inexpensive [56–58]. In the last couple of decades, the exploitation of sunlight for energy production has gained even more attention. At the moment, the only available technologies in the open market are photovoltaics (PV), which are used for electricity production [59,60]. For this reason, the scientific community is actively looking for innovative, sustainable yet efficient processes to convert solar energy into high energy molecules, which are generically called solar fuels. Moreover, Lewis and Nocera have explained why photocatalysis for solar fuels production, can also be thought of as a reliable solution to sunlight intermittency which is an issue in solar energy utilization [61]. In recent years, a great number of papers have been published on these topics, providing either an insight on physicochemical properties of these reactions or technologically advanced materials and photoreactor designs, although the connection between the two topics has not yet been sufficiently highlighted.

For this reason, this review is aimed at summarizing the advancement of the research on the two most promising solar fuel production technologies (i.e., CO_2 photoreduction and photoreforming), providing a comprehensive overview on the most innovative solutions to overcome physicochemical limitations by process design.

2. CO_2 Photoreduction with Water

2.1. Proposed Reaction Pathways

The first study on photoelectrocatalytic carbon dioxide reduction using semiconductors was reported by Inoue and co-workers in 1979 [62]. Irradiation was used to activate a semiconductor anode which was coupled with a platinum cathode, allowing water oxidation and carbon dioxide reduction. It took only a year from this pioneering result for a published paper on purely photocatalytic CO_2 reduction with water on common semiconductors (such as WO_3, $SrTiO_3$ and TiO_2) [63]. However, the latter approach only became of interest from the late 1990s onwards, when many studies were published on the topic. In all cases, the design of an effective process requires a deep physicochemical knowledge of the reaction.

As with any heterogeneous catalytic process, CO_2 photoreduction also consists of three different steps:

1. Reactants' adsorption and photons absorption on the photocatalyst;
2. Heterogeneously catalysed chemical reaction; and

3. Products' desorption.

The first step is fundamental because it allows both reactants to interact with each other with a suitable orientation for the redox reaction to happen.

When the reaction is performed in water, both as a reductant and a reaction medium, CO_2 solubility in the aqueous phase system must be considered as a possible limiting step for the reaction in the liquid phase whereas in the gas phase, mixability is not an issue to be considered. Gaseous CO_2 adsorption can occur with different geometries, affecting overall process efficiency. In the literature, it is well reported that CO_2 adsorption on titanium oxide is considerably weaker than vapour [64–66]. In fact, CO_2 adsorption on TiO_2 follows a Freundlich model, which is generally used for non-ideal sorption processes [67]:

$$q = k_f p^{1/n} \quad (1)$$

where q is adsorbed gas (mmol of gas/g of adsorbent), p is pressure ad equilibrium, while k_f and n are Freundlich constants. The calculated $1/n$ value, 0.4, indicates that the predominant CO_2 adsorption mechanism is chemical adsorption rather than physical adsorption.

Unfortunately, Krischok et al. observed that when CO_2 and water competitive adsorption occurs, CO_2 adsorption was blocked by the presence of pre-adsorbed water on the titanium dioxide surface while weakly adsorbed CO_2 was displaced by post-dosed H_2O, and there was little evidence of bicarbonate formation in either case [68]. Tan and co-workers calculated adsorption constants for CO_2 and H_2O on graphene oxide modified TiO_2 according to a Langmuir-Hinshelwood model and calculated a value of 0.0193 and 8.070 bar^{-1} respectively, confirming findings from previous research [69].

As observed by Henderson and co-workers for TiO_2 based materials [70,71], oxygen from water coordinates with surface titanium sites, whilst protons interact with bridging oxygen, yielding surface hydroxyl groups, which act as adsorption sites for molecular water [72]. He et al. described several possible configurations of CO_2 and TiO_2 interactions, calculating binding energies by computational models [73]. CO_2 can be linearly adsorbed by Ti-O bonds (Figure 1a) or bidentate chelate-like structures can be observed by the interaction of oxygen atoms in CO_2 with adjacent Ti centres (Figure 1b) or carbonate-like structures can be found when C and O atoms from CO_2 interact with surface Ti and O sites (Figure 1c). According to their calculations, the last two configurations, which involve the weakening of C=O bond, seem to be the most likely intermediate in the reduction route.

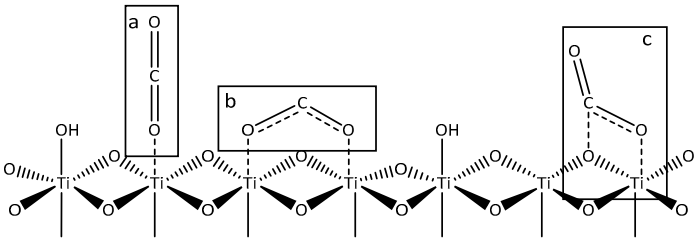

Figure 1. Schematization of interaction between TiO_2 surface and CO_2: linear (**a**), chelate like (**b**) and carbonate like (**c**).

Very recently, Olivo et al., by means of CO_2 adsorption studies using FTIR analyses, observed that all three species are present on metal modified TiO_2, but samples with the highest photocatalytic activity proved to be characterised by the highest share of adsorbed CO_2 in bidentate structures [74].

From all provided evidence, it is clear that CO_2 adsorption on commonly used semiconductors, and titanium dioxide in particular, represents one of the most challenging issues in the development of a photocatalytic process for CO_2 reduction.

Considering the sequent step, i.e., photocatalytic electron transfer, without any catalyst or photocatalyst, reduction cannot happen due to the high energy barrier in the gas phase

(>200 kJ·mol^{-1}) [75]. As reported by Nguyen and Ha from theoretical and spectroscopic studies, CO_2 can interact with water vapour [76]; oxygen lone pairs in H_2O can interact with anti-bonding $2\pi_u$ at central carbon atoms in CO_2, leading to the formation of van der Waals complexes [77].

Despite the great efforts in understanding CO_2 photoreduction by using conventional catalysis tools, the effect of photons has not been successfully described, and due to substantial differences in experimental procedures and reaction regimes, it is difficult to compare data and assumptions from different teams. UV light is more commonly used than visible light. In fact, bare titanium dioxide, the most common catalyst, requires in the case of anatase phase, a radiation wavelength equal to or lower than 388 nm [78]. On the Earth's surface, the average irradiance provided by the sun is 1000 W·m^{-2}, but only ca. 5% is UV irradiation [79]. In most reported CO_2 photoreduction tests, energy input is considerably higher that available solar energy. In fact, irradiance value is usually in the range of 1000–3000 W·m^{-2}, which is much higher than the UV light fraction in sunlight [80–83]. Results from tests performed at lower irradiances are reported in only a few papers; for instance, Woolerton et al. performed CO_2 photoreduction tests in the aqueous phase under 450 W·m^{-2} irradiance [84], whilst more recently Tahir et al. reported tests conducted at 200 W·m^{-2} in the vapour phase conditions [85]. Nonetheless, at the moment, papers reporting CO_2 photoreduction tests using an irradiance below this value are very rare [86,87].

Reactions involved in all semiconductors' light harvesting indicate that a high photons input, from a kinetic point of view, enhances the formation of photocatalytically active sites (Equation (2)) [88].

$$TiO_2 + h\nu \rightleftharpoons h^+_{VB} + e^-_{CB} \quad (2)$$

However, the reverse reaction can also happen, and according to Liu and Li [89], the recombination rate of e^-–h^+ pairs is nearly two or three orders of magnitude faster than the rate of charge separation/transport and chemical reaction itself. Therefore, at high irradiance conditions, where the surface is saturated with photons, the rate of charge carrier recombination becomes higher than both light adsorption and surface reaction rates [90]. Despite these general considerations, there are no specific guidelines for photons' absorption for CO_2 photoreduction. In fact, only Tan et al. have reported the effect of irradiance on methane formation [69]. In their paper, they reported that between 650 W·m^{-2} and 1800 W·m^{-2}, which is a much higher range than the one considered in this part of the work, methane production increased with irradiance. However, the growth was not linear and the subject was not further investigated.

Electronic transfer is of great importance in CO_2 photoreduction, since desired product formation requires more than two electrons transfer. In addition, according to Rasko and Solymosi, this step determines overall kinetic rates of the process [91]. On the contrary, from a thermodynamic point of view, considering reduction potentials, reported in Table 1, methane formation is the most favoured among the C_1 products due to its less negative potential [92].

Table 1. Electrons required to reduce CO_2 to C_1 hydrocarbons [92,93].

Products	Electrons to Obtain Product from CO_2 Reduction	Redox Potential (eV)
CO	2	−0.53
HCOOH	2	−0.61
HCHO	4	−0.48
CH_3OH	6	−0.38
CH_4	8	−0.24

However, kinetic insights on this process are not unanimous; different reaction mechanisms have been proposed for this reaction according to different experimental parameters, such as developed catalyst, irradiation source and reaction medium [64,88,89,94]. All proposed mechanisms describe similarly what occurs in oxidative sites on the photocatalyst surface; valence band's (VB) electron

deficiency, induced by sufficiently energetic incident irradiation, is responsible for water oxidation to molecular oxygen [95,96]. On the contrary, the phenomena involved in the reduction process in the conduction band (CB) have not been clarified yet.

In 1995, Anpo et al. for the first time proposed a reaction mechanism for CO_2 photoreduction: XANES, EXAFS and photocatalytic tests indicated that CO_2 reduction occurs on $(Ti^{3+}–O^-)^*$ transient species via C=O cleavage and O_2 desorption and subsequent hydrogenation of remaining C surface species with H and OH surface species, without further details on the reducing species. Later, Dimitrijevic et al. used EPR studies to confirm the formation of the common intermediate for any product is CO_2^- radical anion, which is bound on the TiO_2 surface [97], as previously observed by Tanaka and co-workers on MgO [98,99]. In the literature, several authors confirmed that the first step is the formation of peroxocarbonate species, which are reduced to formic acid, formaldehyde, and methanol afterwards [89,100,101]. Nonetheless, over the last decade, due to the growth in the processes and catalysts developed, a single mechanism cannot be assumed because a variety of reaction pathways can occur according to reaction conditions and catalysts [89,95].

According to CO_2 photoreduction tests performed in aqueous phase, as reported by Liu and Li [89], the presence of peroxide species in water were hypothesised; but, being characterised by a high redox potential, they are extremely unstable, and thus, unreliably detectable. Therefore, peroxocarbonate species are the first intermediates, then, they are directly converted into formate ions, formic acid, and further reduction products. However, formaldehyde is the first product formed when basic aqueous solutions are adopted, and further reduction to methanol or oxidation to formic acid may occur.

According to Galli et al., wide product distribution in liquid phase tests indicates that CO_2 photoreduction occurs by consecutive reaction steps at neutral pH [102] (Equations (3)–(8)).

$$\text{VB}: \ 2H_2O + 4h^+ \rightarrow 4H^+ + O_2 \tag{3}$$

$$\text{CB}: \ H^+ + e^- \rightarrow \cdot H \tag{4}$$

$$CO_2 + 2 \cdot H \rightarrow HCOOH \tag{5}$$

$$HCOOH + 2 \cdot H \rightarrow HCHO + H_2O \tag{6}$$

$$HCHO + 2 \cdot H \rightarrow CH_3OH \tag{7}$$

$$CH_3OH + 2 \cdot H \rightarrow CH_4 + H_2O \tag{8}$$

Due to the high H_2O/CO_2 ratio in liquid phase systems, CO_2 undergoes hydrogenation faster than deoxygenation, leading to all oxygenated products found in reaction medium. However, it was observed that TiO_2 catalyst modification with metal electron traps increases hydrogenation rate and improving methane yield by enhancing the stability of electron-hole couples [103,104].

Furthermore, the accumulation of organic compounds in the liquid phase can be followed by hydrogen formation by PR; produced organic compounds act as hole scavengers themselves in a PR reaction (Equation (9)). This reaction is very likely to happen with methanol due to its reactivity compared to other C_1 compounds [105,106].

$$CH_3OH + H_2O \rightleftharpoons CO_2 + 3H_2 \tag{9}$$

On the contrary, CO_2 photoreduction can also be performed in the gas phase, feeding water as vapour, leading to slightly different results in observed mechanisms. For example, Karamian and co-workers [88] reported that in most cases, in gaseous systems CO is the first intermediate product of CO_2 photoreduction by water vapour [74].

$$CO_2 \rightarrow CO + O_2 \tag{10}$$

Generally speaking, in the gas phase deoxygenation is faster than hydrogenation and it leads to ·C species that are reduced afterwards, whereas in the liquid phase, peroxo species undergo hydrogenation preferentially [107], yielding to possible intermediate products. However, reaction conditions, and in particular, temperature, irradiance, and reaction time modify the reaction pathway and product distribution as a consequence. In detail, if CO_2 deoxygenation is faster than dehydrogenation, methane production is favoured with respect to oxygenated compounds [94]. This is the case for the vapour phase reaction, characterised by CO_2 excess. This mechanism involves the formation of ·C radicals that recombine with ·H originated from water [108].

From all the evidence reported in the literature, briefly summarized in Table 2, it is possible to assume that CO_2 reduction can undergo two different pathways, as shown in Figure 2.

Table 2. Summary of proposed mechanisms found in the literature.

Ref.	Catalyst	Reaction Conditions	Products Formation	Notes
[64]	Anatase TiO_2	- CO_2 0.04–0.15 mmol - H_2O 0.04–0.25 mmol - UVA lamp - 0–50 °C, 1 atm	CH_4 0.17 μmol·g^{-1}·h^{-1} H_2 8.33 μmol·g^{-1}·h^{-1}	- C=O cleavage to form C species, which interact with H atoms and OH radicals
[110]	TiO_2 (P25)	- CO_2 2.8 MPa - 0.1 M i-PrOH in H_2O as hole scavenger - UVA lamp - 20 °C, 2.8 MPa	CH_4 1.2 μmol·g^{-1}·(Ti) energy efficiency 0.0065%	- i-PrOH improved methane production by enhancing H^+ formation
[111]	$Pt/CuAlGaO_4$ $Pt/SrTiO_3$ WO_3	- 2 mM $FeCl_3/FeCl_2$ with Nafion membrane - CO_2 dissolved - 300 W Ne lamp 270 mW·cm^{-2} - pH 2.6, r.t. and 1 atm	CH_3OH 473.3 μmol·h^{-1}	- dividing oxygen and hydrogen improves methanol yield
[112]	TiO_2	- 0.08 M $NaHCO_3$ - 500 W Xe lamp - r.t., 1 atm	CH_3OH 0.59 μmol·g^{-1}	- CO_3^{2-}/HCO_3^- reduction improved by catalyst charge separation on the catalyst
[102]	TiO_2 (P25)	- 1.7 g·L^{-1} Na_2SO_3 + 11 g·L^{-1} NaOH - pressurised CO_2 - 104.2 W·m^{-2} - pH 14, 80 °C, 7 bar	CO 0.72 μmol·g^{-1}·h^{-1} HCOOH 1859 μmol·g^{-1}·h^{-1} HCHO 16,537 μmol·g^{-1}·h^{-1} CH_3OH 351 μmol·g^{-1}·h^{-1}	- pressure improves CO_2 solubility in reaction medium - two parallel reaction pathways are hypothesized
[113]	Cu/TiO_2	- CO_2 + H_2O gaseous mixture 2 mL·min^{-1} - 150 W lamp 90 mW·cm^{-2} - r.t., 1.5 bar	CO 25 μmol·g^{-1} CH_4 4 μmol·g^{-1}	- The first step is CO_2 splitting into CO and O_2
[81]	Cu/TiO_2	- CO_2 + H_2O gaseous mixture - optical fibres lamp (λ = 365 nm) 1–16 W·cm^{-2} - 75 °C, 1.05–1.40 bar	CH_3OH 0.4 μmol·g^{-1}·h^{-1}	- Kinetic studies indicate that the redox reaction is the rate determining step of the process (not adsorption nor desorption)
[114]	Montmorillonite/TiO_2 monolith	- CO_2 + H_2O gaseous mixture (1.4 bar) - 200 W Hg lamp - r.t., 1.4 bar	CH_4 139 μmol·g^{-1}·h^{-1}	- Reaction occurs via multiple single-electron transfers - Bimolecular Lagmuir-Hinshelwood model
[115]	SO_4^{2-}/TiO_2	- CO_2 + H_2O + H_2 + N_2 gaseous mixture - low pressure Hg lamp (λ = 365 nm) 2.0 mW·cm^{-2} - 35–85 °C, 101.3 kPa	CO 0.85 μmol·g^{-1}·h^{-1} CH_4 0.14 μmol·g^{-1}·h^{-1}	- Oxygen formation retards CO_2 reduction
[69]	Graphene oxide/TiO_2	- CO_2 + H_2O + N_2 gaseous mixture (25–101 kPa) - Xe lamp (AM 1.5) 65–177 mW·cm^{-2} - 25 °C, 1 bar	CO 14.91 μmol·g^{-1} CH_4 3.98 μmol·g^{-1}	- adsorption of water is 10 times faster than carbon dioxide - proposed mechanism include only CO and CH_4 as products

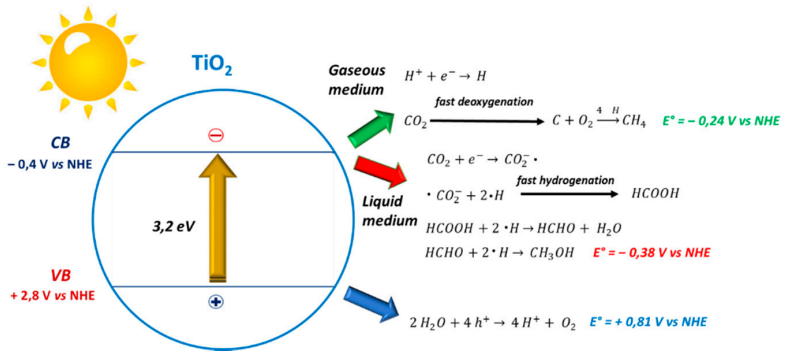

Figure 2. Different reaction mechanisms in the vapour and liquid phases. CB and VB energy levels have been taken from [109].

Once reagents are turned into products, they need to be desorbed from the catalytic surface so as to leave catalytic sites available for new reagents' molecules to be adsorbed.

2.2. Photoreactor Design

The choice of the reactor design and process conditions heavily affect substrate and photon delivery to the photocatalytic surface. While mass transfer is commonly considered in conventional catalysis processes, in photocatalysis, photon transfer must be addressed too. Due to the novelty of this technology and the increase in publications on this topic, different rig configurations are reported in the literature. In fact, if we consider reported photoactivity data for a worldwide benchmark photocatalyst, such as Evonik's P25, with the same conditions of temperature, pressure and light intensity, performances might change either in terms of activity and product distribution [92,116,117]. In the first studies, three-phase photoreactors (solid catalyst, liquid reaction medium, gaseous CO_2) are generally reported [62]. In this case, the solvent, which is water, acts as a reductant as well [118], therefore, several phenomena should be considered for mass transfer such as solubility, diffusion, convection and migration. CO_2 solubility in an aqueous phase system must be considered as a possible limiting step for the reaction in the liquid phase.

From an historical point of view, the first developed photoreactors for CO_2 reduction were batch reactors where the catalyst was suspended in a liquid medium, usually water, and carbon dioxide was bubbled through reaction medium and light reached the reaction medium through quartz windows [62,119–121]. This choice of three-phases slurry reactors was, and still is, widely used due to many advantages. These experimental rigs are similar to those used for carbon dioxide photoelectrocatalytic reduction [122,123], and most importantly, they have been widely used in photooxidation processes, which in some cases, are available on a commercial scale [124,125].

In addition, the catalyst does not require any casting or shaping procedure before its use so it can be used as a powder without further modification. Mass transfer is achieved by mixing, either magnetically or mechanically, to provide homogeneity in the reaction medium.

However, liquid phase setups are affected by experimental drawbacks that need to be overcome. The two main drawbacks to be overcome are extremely low carbon dioxide solubility in water (0.03 M at 25 °C and 1 atm) [126], and inefficient light harvesting by medium scattering [127,128]. The most common strategy to solve the first problem is the introduction of a base to improve CO_2 solubility. Many authors use basic solutions as reaction media, which leads to the formation of more soluble and stable carbonates and bicarbonate species in the solution [129]. Generally, the most used base is sodium hydroxide [130,131], but use of other bases is reported, such as sodium bicarbonate [132], potassium biphosphate [133] and triethanolamine (TEA) [134].

Quin and co-workers did not use water as a reaction medium, but used methanol, whose CO_2 solubility is much higher [135], and they observed that the main product was methyl formate which was obtained by esterification of the solvent and formic acid from CO_2 reduction. Alternatively,

Liu and co-workers used isopropanol as a solvent, increasing CO_2 solubility and leading to similar results [136]. However, it has been observed that these solvents can act as sacrificial agent and be oxidised in TiO_2's valence band instead of water [111]. This means minor sustainability of the process because in these photocatalytic systems, the reductant is more expensive and industrially derived from fossil sources (mainly natural gas or coal gasification).

Rossetti et al. reported that the use of a pressurised photoreactor increased CO_2 dissolution in aqueous media, yielding higher catalytic activity in methane production avoiding chemical absorption as carbonates in high pH conditions [87], which might lead to reactor walls corrosion. Indeed, the increase in pressure enhances carbon dioxide dissolution in reaction medium to increase reduction products and overall process productivity, but it was observed that reaction thermodynamics hindered photocatalytic performances for values higher than 10 bars [137]. Even tuning temperature represents a challenge, since its increase positively influences kinetics and mass transfer, but it reduces CO_2 solubility and favours electron-hole recombination. Kaneco and co-workers performed photoreduction in liquid CO_2, overcoming solubility problems [138] at 20 °C, but, compared to common photocatalytic reactions, pressure is extremely high (6.5 MPa) in order to maintain CO_2 in the liquid phase.

The second issue to face in three-phase batch reactors is light transfer. In fact, photons are required to travel from light source through reaction medium to the photocatalyst surface, where they are absorbed and activate the photocatalyst. At 20 °C and with 361 nm light wavelength, the water refractive index is 1.34795, whereas the refractive index value is 1.000464 for CO_2 and 1.000256 for water vapour [126,139]. This means that light transfer in aqueous solutions is much more difficult in liquid media compared to gas phase systems.

For light harvesting, a variety of photoreactors geometries aimed at maximising catalyst photoactivation, were reported. In the liquid phase, the most commonly-used systems feature a quartz window that allows light to enter [64,140,141]. More recently, some papers in the literature have reported the use of an annular design that allows a homogeneous light transfer to the catalyst, mainly in the radial direction [142]. For example, Matějová and co-workers used a batch reactor with this geometry: the UV lamp is cast at the centre of the reactor to maximise light harvesting efficiency and it irradiates the aqueous catalyst suspension and CO_2 is bubbled through it to reach saturation, as depicted in Figure 3 [107].

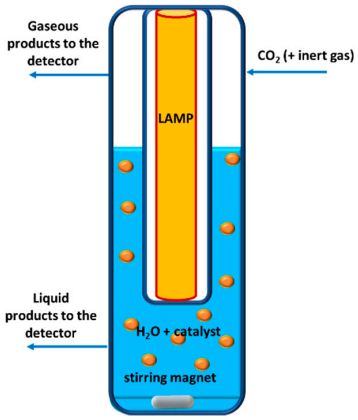

Figure 3. Example of a three-phase photoreactor for CO_2 photoreduction.

Finally, the use of a fine suspended catalyst might lead to fouling of radiation source, lower active surface contact area and higher separation cost for product collection. Despite technological advances, some of these issues such as high refractive index and poor solubility cannot be completely eliminated, reducing the potentialities of these systems.

Over the years, gas-solid photoreactors have become popular in the literature. This solution finally provides a solution for issues related to CO_2 solubility in water. In fact, as any gas, water vapour and CO_2 are perfectly mixable and water vapour diffusion in CO_2 constant is relatively high

(0.138 $cm^2 \cdot s^{-1}$); thus, it is possible to tune reactants' ratio and perform photoreduction in CO_2 excess while avoiding water splitting. Moreover, separation is easier since reagents and products are in gas phase while the catalyst is solid.

Mixing the reagents can be performed using different physical phenomena and technological solutions, which differ in their control of the CO_2/H_2O ratio. Bazzo and Urawaka reported the use of moist quartz wool to generate water vapour in situ [143]; vapour feed control was not precise leading to errors in CO_2/H_2O ratio calculations. Collado and co-workers used a controlled evaporator mixture to maintain reactants ratio [144] whilst other researchers, such as Tahir and Amin [145] or Cybula et al. [146] employed a water bubbler to saturate flowing CO_2 with water vapour, as reported in Figure 4. In this way, it is possible to tune the water amount controlling temperature, pressure and carbon dioxide flow. However, in the reported papers temperature is not controlled, though it affects water vapour pressure and thus CO_2/H_2O ratio, decreasing the tests reproducibility.

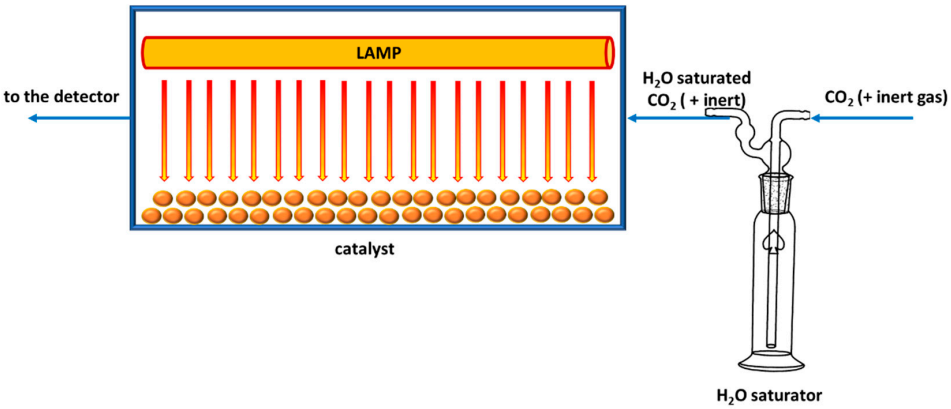

Figure 4. Example of a photoreactor for gas-solid CO_2 photoreduction where a water saturator is employed.

Gas-solid systems also allow a great choice of catalyst introduction techniques. Packed bed reactor design is the easiest technological solution, since low pressure drops can be achieved, controlling catalyst particle size and providing promising results [147]. However, it suffers from a low irradiated surface area to volume ratio that negatively affects photon harvesting, and thus, light absorption and scattering [148]. According to Kočí and co-workers [149], an annular reactor, where the catalyst is embedded within two concentric cylinders and the radiation source is in the centre, improved irradiation homogeneity, despite issues with gases mixing due to small cross-section.

To overcome inhomogeneous irradiance, several solutions have been developed. The use of optical fibres instead of a single light source provides high transmission and irradiation uniformity [150]. This kind of irradiation is generally coupled with the use of honeycomb monoliths, which also minimise pressure drops. The catalyst is layered within monolith inner walls by wash-coating or, as reported by Ola and Maroto-Valer [151], it is synthesised in situ by a sol-gel method. However, in these systems, mass transfer of reagents and products to and from the catalytic sites might be too critical and channel opacity might decrease light harvesting efficiency [152].

Finally, another possibility for gas-solid reactors is thin film reactors. In this configuration, the photocatalyst is not immobilised onto beads, fibres or monoliths, but it is deposited on a plate, or even better, on the surface of the photoreactor. In this case, irradiation and light distribution are influenced by geometry and light source with significant effects on global photoactivity [153]. Several geometries were reported in the literature, for example, Pathak et al. used Nafion membranes to support photocatalyst film [154] whereas Tan and co-workers used a quartz rod within the photoreactor [69].

Ideally, a solar light driven photoreactor must have [129]:

- high coverage area and homogeneous catalyst distribution with good exposure to light;

- high CO_2 velocity and high mass transfer;
- intimate contact between reagents, catalyst and photons;
- efficient light harvesting.

Comparing both photoreactors (whose features are summarised in Table 3), gas-solid systems are the most promising option for the design of a photoreactor due to their flexibility in process development and fewer limitations due to mass-related physical phenomena (i.e., CO_2 adsorption and light scattering through reaction medium).

Table 3. Summary of features to consider in CO_2 photoreactor design.

Type of Photoreactor	Issue	Approach
Three-phase photoreactors	CO_2 solubility	Basic reaction medium Alternative solvent High Pressure
	Water splitting	Sacrificial Agent
	Light scattering	Efficient stirring Wise reactor geometry
	Fouling	Preformed Catalyst
	Separation	Preformed Catalyst
Gas-Solid photoreactors	Variable CO_2/H_2O ratio	Control of reactants feed
	High contact time	Bath reactor
	Irradiation inhomogeneity	Geometry Optic fibres Catalyst immobilisation

Considering reactants feed, bubbling gaseous CO_2 seems the easiest most efficient way to obtain CO_2-rich reactant mixtures, avoiding the use of sacrificial agents, although it is possible to obtain a stable and constant CO_2/H_2O ratio with careful control of CO_2 flow and bubbler temperature.

3. Photoreforming of Biomass-Derived Substrates

3.1. Proposed Reaction Pathway

Reforming processes and in particular PR, as shown in the introduction, could be a very promising answer for both low-cost hydrogen production and storage. Nonetheless, hydrogen can also be produced from pure water through so-called photocatalytic water splitting [155]. As pointed out by Ma et al. [156], a lot of papers make claims about "water splitting" while using a so-called hole scavenger [157]; but since no oxygen is evolved in this case, it is more proper to term these reactions as photoreforming or partial water splitting [156]. Despite its attractiveness, this reaction is more difficult than PR, both from a thermodynamic and kinetic point of view, leading to lower hydrogen productivity [158].

The effect of these hole scavengers, or sacrificial reagents, as boosting agents in photocatalytic hydrogen production from water was first observed by Kawai and Sakata in 1980 [159]. Today several compounds are known to be effective in PR with methanol [160], ethanol [161] and glycerol [162] being the most used.

The general mechanism of photocatalysis has been widely described by several authors [46,156]. Briefly, upon absorption of a sufficiently energetic photon, charge carriers, unless they recombine, can be transferred to a suitable electron acceptor (for electrons) or donor (for holes) [163]. CB energy should be higher than the acceptor while VB energy should be lower than the donor, so that reaction can occur [46]. In a PR reaction, the acceptor is a hydrogen ion, yielding molecular hydrogen (H_2), while the donor, previously labelled as a hole-scavenger, is the reducing agent, either inorganic [164]

or organic [165]. For the oxidative reaction pathway that consumes the hole scavenger, two main pathways have been proposed, depending on the water/substrate ratio [166]:

- Direct path, consuming the substrate directly by holes;
- Indirect path, a hydroxyl radical-mediated mechanism, where these radicals are produced by interaction of holes with adsorbed water or surface hydroxyl moiety.

Beside these two main pathways, a deeper understanding of degradation mechanism is useful. A general mechanism scheme is reported in Figure 5, as proposed by Puga [46].

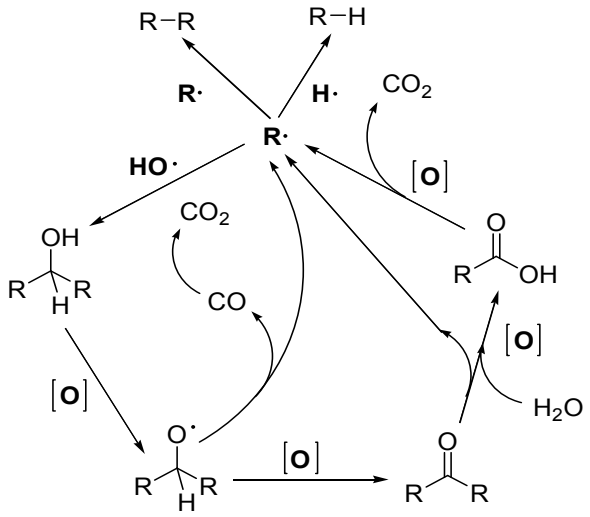

Figure 5. General proposed mechanisms of oxygenates PR (oxidative pathway).

It has been proposed that alcoholic moiety, one of the most abundant oxygen-containing functional groups in biomass, undergoes consecutive oxidation to carboxylic acid, eventually decomposing to an alkyl fragment or radical and carbon dioxide (decarboxylation) [167]. Nonetheless, this mechanism seems to only be logical for polyols; ethanol is known to yield acetaldehyde as its main co-product [168–170], suggesting a key role played by the substrate's structure in enhancing C-C bond cleavage. Besides this mechanism, an alternative pathway was proposed by Bahruji et al. on Pd/TiO_2 where alcohol was adsorbed as alkoxide, then decarbonylation yielded an alkyl fragment and CO, which further oxidized to CO_2 by holes [171]. Concerning the as-formed alkyl fragments, several pathways have been proposed, for example, recombination with either hydrogen atoms or other alkyl fragments yields hydrocarbons [172], while coupling with hydroxyl radicals gives alcohols [173], that can be further oxidised until complete mineralization of the carbon skeleton to CO_2. This suggests a higher availability of these radicals improves substrate degradation. Finally, unexpected by-products suggest other side-pathways such as etherification and esterification [174], ketonisation [175], radical coupling [176] and hemiacetalisation [168].

Thus, the reaction mechanism is a complex phenomenon, strongly substrate and catalyst-dependent. Nonetheless, the key point of reaction pathway knowledge is to understand how by-products are produced and how these side processes can be correlated to catalyst and reaction conditions, as will be explained in the following sections.

3.2. Catalyst Formulation

The ideal photocatalyst should be selective to complete organics mineralisation, stable and as cheap as possible in order to be applied on an industrial scale. The greatest challenge for a photocatalyst is strong visible light absorption and high carrier mobility (i.e., reduced recombination) [177] in order to harvest solar light efficiently. Moreover, visible light absorption allows lower energy losses since the energy required to excite the photocatalyst exceeds the thermodynamic requirements of

reforming [178]. Concerning photocatalytic material properties, little attention has been focused on important parameters such as band edges, optical absorbance and carrier mobility [177]. Knowledge of these properties is important for efficient light harvesting and utilisation.

TiO_2 is certainly the most studied and well-known material in photocatalysis due to its inexpensiveness, safety, chemical stability and photostability [156,179]. TiO_2 aside, different materials have been reported such as zinc oxide (ZnO) [180], copper oxides (CuO and Cu_2O) [181], strontium titanate ($SrTiO_3$) [182], sodium tantalate ($NaTaO_3$) [183], indium tantalate ($InTaO_4$) [184], cadmium sulphide (CdS) [185], tantalum nitride (Ta_3N_5) [186], tantalum oxynitride (TaON) [187], graphene [188] and carbon nitride (C_3N_4) [189]. Besides pure materials, solid solutions have also been used to tune the band structure and improve visible light absorption. Examples include bismuth-yttrium vanadate ($Bi_xY_{1-x}VO_4$) [190] and zinc-cadmium sulphide ($Zn_{0.5}Cd_{0.5}S$) [191]. In order to improve the catalytic activity of pristine material, several strategies have been widely reviewed in the literature [57,156], targeting visible light harvesting, reducing electron-hole recombination and improved reaction kinetics. Such approaches include nanostructure architecture [180,192–194], doping [193,195,196], heterojunction [197–203], use of plasmonic metals [186,204,205], as well as co-catalysts [164,206,207]. Concerning nano-composites (joining of two or more materials at nanoscale), an interesting concept is the so-called Z-scheme. Bard suggested the first mechanism proposal of this system in 1979 [208] and the first all-solid-state Z-scheme system for overall water splitting, was developed by Sasaki et al. [209]. As pointed out by Zhou et al., it involves the transfer of an electron from the lowest-lying VB to the highest-lying CB of the composite, thus gaining in reactivity for both electron and holes compared to heterojunctions [210]. Few Z-scheme systems have been stated for PR [211,212], but very appealing systems are reported in the literature, such as $CdS/Au/WO_3$ [194] and $g\text{-}C_3N_4/WO_3$ [213]. These nano-composites are able to fully harvest visible light, while exploiting high-reactive charge carriers for photocatalytic reactions, as pictured in Figure 6. Due to great potentiality of Z-scheme systems and the wide variety of available semiconductors [177,210], a lot of work can be done on assessing diverse materials on their nano-composites' photocatalytic properties.

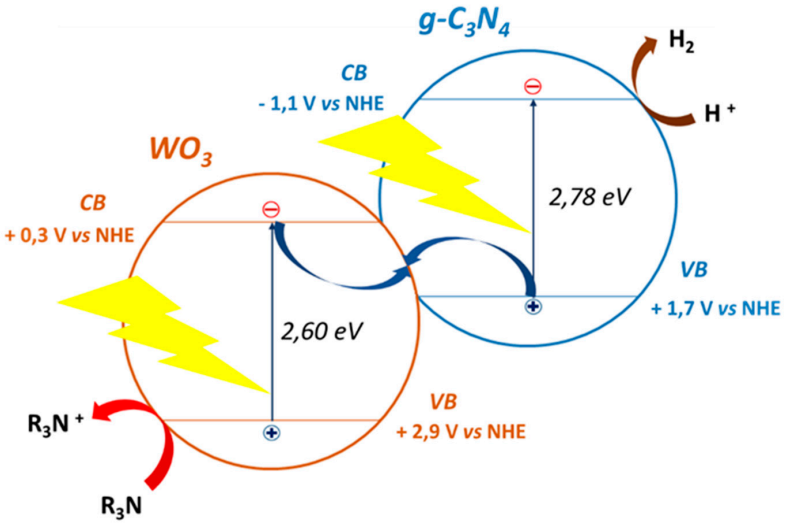

Figure 6. Z-scheme of visible light harvesting $g\text{-}C_3N_4/WO_3$ nano-composite. CB and VB energy levels have been taken from [213].

Among the other approaches mentioned above for activity enhancement, the use of co-catalysts is an appealing method, in particular, by improving reaction kinetics [214]. An increase in hydrogen evolution up to 2–3 magnitude order compared to pristine material has been reported [215,216]. The role of co-catalysts is to trap excited electrons [217] or, less commonly, holes [218], and act as a reaction site [214]. Reduction co-catalysts are the most used to increase catalytic activity and usually

rely on noble metals such as gold (Au) [168,219], platinum (Pt) [193,220] and palladium (Pd) [171]. Chiarello et al. observed increased reactivity upon co-catalysts loading, in order, Ag < Au < Pt, explained by their increasing work function, and thus electron-trap capability [174]. Al-Azri et al. found an increase in activity, in order, Au < Pt < Pd, suggesting the higher reactivity of Pd is due to higher Fermi level and density of states despite it having a lower work function than Pt [178]. Besides expensive noble metals, non-noble ones have been evaluated too. Copper (Cu) [170] and nickel (Ni) [221,222] have proved to be as active as noble metals in improving photocatalysts' activity. Metal oxides such as copper(II) oxide (CuO) [216,223], nickel oxide (NiO) [224] and cobalt oxide (CoO_x) [164] have also been reported to be suitable co-catalysts, although NiO has been proved to be converted in situ in metallic Ni, the truly active phase [222]. Ni and Cu-based co-catalyst are surely the most reported [46], but cobalt-based materials also show interesting activity in hydrogen evolution [225] even though they are scarcely reported in literature. Moreover, few comparisons among these non-noble metal co-catalysts exist. Fujita et al. reported an increased reactivity, in order, CoO_x < NiO < CuO on TiO_2 [226], while Sun et al. observed an improved hydrogen evolution, in order, RuO_x < NiO < CuO < CoO_x < Pt on a barium titanate [158], suggesting that interactions between the co-catalyst and the main semiconductor play a crucial role too. Alloying has been proved to boost the catalytic activity [227–229], probably due to synergistic effects among the two components as suggested by Jung et al. [230]; unfortunately, these reported alloys contain at least one noble metal, increasing the cost of the catalyst. Further work on purely non-noble metal alloys is necessary to gain a comprehensive knowledge of alloyed co-catalysts. Interesting alternatives to metal and metal oxides are metal sulphides, such as molybdenum disulphide (MoS_2) [231,232] and tungsten disulphide (WS_2) [233,234]; Zong et al. demonstrated a higher activity of MoS_2 compared to noble metals on CdS photocatalyst [235]. Oxidation co-catalysts are widely studied for overall water splitting [155], and compared to oxide co-catalyst (RuO_x, IrO_x, CoO_x), cobalt phosphate (Co-Pi) has been reported to obtain higher activity in oxygen evolution [236] and to also exhibit self-healing properties in the presence of phosphate ions in solution, thus improving its stability [237]. Recently, Di et al. reported an enhancing of activity in PR with Co-Pi co-catalyst, thus boosting the oxidative side of the reaction mechanism [238]. Beyond the choice of the material, the loading is also important. Usually a very low amount of co-catalyst is able to boost the activity, for instance Kondarides et al. assessed 0.1–0.5% as the optimal Pt loading on TiO_2 [162] while Chen et al. estimated that 1.25% of CuO [223] and 0.5% of Ni [222] gave the best result on TiO_2. Increasing the loading certainly increases the number of available active sites, but above a certain upper value the activity decreases due to enhanced charge carrier recombination, light-shielding effect or the decrease of active sites at the metal-semiconductor interface [162]. Besides activity enhancement, the co-catalyst plays a significant role in selectivity [174,239], moreover, its size has been proved to have a remarkable role in enhancing both activity and selectivity of PR reactions [240]. Finally, as reported by Kawai and Sakata in 1980 [159], the use of two co-catalysts (for both reduction and oxidation half-reactions) could remarkably improve photocatalytic performance, thus, suggesting further development on this side.

In Table 4 some of the most interesting used photocatalysts are summarized, reporting reaction conditions and product formation.

Table 4. Summary of some used photocatalysts for biomass PR.

Ref.	Catalyst	Co-Catalyst	Reaction Conditions	Products Formation	Notes
[168]	TiO_2	1.0% Au	- 50:50 *v*/*v* EtOH/H_2O - 1 g/L of catalyst - UV light (125 W) - 20 °C and 1.4 bar - 2 h of reaction	H_2 11,242 μmol·g^{-1}·h^{-1} CH_4 88 μmol·g^{-1}·h^{-1} C_2H_4 110 μmol·g^{-1}·h^{-1} C_2H_6 7 μmol·g^{-1}·h^{-1} CO 36 μmol·g^{-1}·h^{-1} CO_2 52 μmol·g^{-1}·h^{-1} CH_3CHO 8258 μmol·g^{-1}·h^{-1}	-
[220]	TiO_2	0.3% Pt	- Olive mill wastewater (OMW) (3.3% *v*/*v*) - pH 3.4 - 4 h of reaction - 2 g/L of catalysts - UVA light; 5.8 × 10^{-7} mol photons·s^{-1}	H_2 183 mol_{H_2}·mol_{Pt}^{-1}	- uncomplete mineralization of OMW - catalyst regeneration by photooxidation - improved H_2 yield by removing lipids from OMW
[171]	TiO_2	0.5% Pd	- 0.1% *v*/*v* alcohols/H_2O - 2 g/L of catalyst - simulated solar light - 3 h of reaction	- 12 mL H_2 (glycerol) - 8 mL H_2 (glucose) - 4 mL H_2 (sucrose) - 2 mL H_2 (cyclohexanol)	- improved H_2 yield with number of α-H in alcohol molecule - observed alkanes as side-product
[170]	TiO_2	0.5% Cu0.5% Au	- 1.5% EtOH and 19% H_2O on inert gas stream - simulated solar light, 1000 W/m^2 - 60 °C - 100 mg of catalyst immobilized on 10 cm^2 of conducting glass substrate	*0.5% Au/TiO₂* H_2 212 μmol·h^{-1} CH_4 8.4 μmol·h^{-1} CO 11.8 μmol·h^{-1} CO_2 7.8 μmol·h^{-1} CH_3CHO 181 μmol·h^{-1} *0.5% Cu/TiO₂* H_2 186 μmol·h^{-1} CH_4 6.9 μmol·h^{-1} CO 9.8 μmol·h^{-1} CO_2 5.5 μmol·h^{-1} CH_3CHO 162 μmol·h^{-1}	- co-catalysts introduced by photodeposition - reaction in dynamic conditions (5 mL/min gas flow)
[216]	TiO_2	0–9% CuO	- 0.1 M glycerol in H_2O - UVA LED (365 nm); 800 W/m^2 - 1 g/L of catalyst	H_2- - from 15.9 μmol·g^{-1}·h^{-1} (0% CuO) to 2061 μmol·g^{-1}·h^{-1} (1.3% CuO)	- linearly decrease of organic in solution (8 h of irradiation)
[222]	TiO_2	0–4% Ni	- 10:90 and 80:20 *v*/*v* EtOH/H_2O - UVA light; 65 W/m^2 - 0.325 g/L of catalyst	*10:90 EtOH/H₂O* H_2 11.6 μmol·g^{-1}·h^{-1} (0.5% Ni/TiO_2) *80:20 EtOH/H₂O* H_2 20.7 μmol·g^{-1}·h^{-1} (0.5% Ni/TiO_2)	- improved H_2 yield by reduction of NiO to Ni
[164]	CdS/TiO_2	0–2.8% CoO_x	- 0.125 M Na_2S and 0.175 M Na_2SO_3 in H_2O - visible light (λ > 400 nm) - 0.5 g/L of catalyst	H_2 660 μmol·g^{-1}·h^{-1} (2.1% CoO_x/CdS/TiO_2)	-
[238]	CdS	0–20% Co-Pi	- Lactic acid in H_2O - visible light (λ > 420 nm) - 0.625 g/L of catalyst	H_2 - from 5.2 mmol·g^{-1}·h^{-1} (0% Co-Pi) to 13.3 mmol·g^{-1}·h^{-1} (10% Co-Pi)	- improved catalyst stability with loading Co-Pi

Table 4. *Cont.*

Ref.	Catalyst	Co-Catalyst	Reaction Conditions	Products Formation	Notes
[194]	CdS-Au-WO_3	-	- 0.2 M Na_2S and 0.2 M Na_2SO_3 in H_2O - visible light (λ > 420 nm) - 0.2 g/L of catalyst	H_2 - 34.6 μmol·h^{-1} (CdS-Au-WO_3) - 16.5 μmol·h^{-1} (CdS-Au) - 6.3 μmol·h^{-1} (CdS- WO_3) - 4 μmol·h^{-1} (CdS)	- WO_3 photonic crystal; Z-scheme system
[213]	g-C_3N_4-WO_3	1% Pt	- 10% *v*/*v* TEOA/H_2O - simulated solar light - 0.625 g/L of catalyst	H_2 - 0.44 mmol·g^{-1}·h^{-1} (Pt/g-C_3N_4) - 3.12 mmol·g^{-1}·h^{-1} (Pt/g-C_3N_4/WO_3)	- Z-scheme system

The key point of this section is that coupling two different materials is necessary in order to fulfil the requirement discussed at the beginning of this section. In this context, co-catalysts play a crucial role in catalytic activity and selectivity enhancement.

3.3. Reaction Conditions

Photocatalyst improvement is just part of the story; reaction conditions play an important role in efficiency enhancement of the overall process. Herein, we focus attention on liquid vs gas phase reaction conditions, since, even though some remarkable differences exist, they have scarcely been highlighted in the literature for PR reaction.

Similarly to CO_2 photoreduction, PR has been extensively carried out in the liquid phase [161,162,168,191,216,241]. Gas phase conditions have been barely reported and only volatile compounds such as methane [242,243], methanol [244,245] and ethanol [170,175,246] have been used. Nevertheless, as reported by Ampelli et al., gas phase conditions have several advantages over liquid conditions [170], such as:

- Low light-scattering losses;
- Easier product recovery;
- Avoiding metal-leaching issues;
- Good catalyst exposure to light.

Several other reaction parameters can affect both the activity and selectivity of PR reactions; these will be briefly summarised here, along with the underlying issues and key points.

Since photocatalysis is a light-driven process, the obvious parameters are light wavelength and intensity in both the liquid and gas phase. Concerning the former, it is known that the lower the incoming photon wavelength, the higher the hydrogen evolution rate [247] and the apparent quantum yield (AQY) [243]. This experimental behaviour is unexpected since the as-formed charge carrier experienced a fast thermalisation (a few hundred femtoseconds) [248], losing their extra-energy at the bottom of CB. However, Xu et al. proposed two explanations for faster methanol dissociation on TiO_2 (110) surface: direct injection of electrons in methanol's lowest unoccupied molecular orbital (LUMO), or a phonon-assisted methanol dissociation using energy from thermalisation [249]. Speaking of the latter (light intensity or irradiance), as previously explained in Section 2.1, lower irradiances improve photon utilization and boost AQY. Unfortunately, few reports exists about the effect of light intensity on PR activity [46]; despite this, a wide variety of light intensities have been used from 2 $W \cdot m^{-2}$ [175] to 250 $W \cdot m^{-2}$ [250]. It is worth highlighting that light wavelength and intensity affect the photon utilization efficiency, rather phenomena involving reagents, products or reactions intermediates such as adsorption, desorption or change in activation energy.

Although the energy source in photocatalysis is light, thermal energy can play a significant role within a narrow temperature range (20–90 °C) [46]. It is widely known that a higher temperature increases hydrogen yield for both the gas [175] and liquid phase [162,251] as reaction medium. Concerning the former, Taboada et al. suggested such evidence is due to improved desorption of reaction intermediates [175]. Nonetheless, Caravaca et al. observed that on Pt/TiO_2, methanol reforming occurs without irradiation at temperatures higher than 160 °C, thus suggesting a shift to a pure thermocatalytic process [245].

Substrates and their concentrations strongly influence both activity and selectivity. Several compounds can be used as hole scavengers in PR, but the most interesting are certainly oxygenates organic compounds because they have higher reactivity than hydrocarbons and potentially lower environmental impact (biomass or biomass-derived compounds) [42]. Hydrocarbons and fossil fuels have been used too [173]. Yoshida et al. reported photocatalytic methane conversion that, despite requiring noble metal co-catalyst and high methane-water ratio, successfully yielded hydrogen and CO_2 [242,243]. We have cited this process since it could be an appealing way to move from

traditional thermocatalytic reforming processes to milder and less energy-demanding PR processes on well-established fossil fuel-based technologies.

Concerning oxygenates, methanol, ethanol and glycerol are certainly the most used as mentioned in Section 3.1. Focusing on the relationship between substrate structure and hydrogen evolution activity, Chen et al. observed, using a Pd/TiO_2 catalyst, increased reactivity with an increasing number of hydroxyl moiety and α-hydrogen on the substrate, and reported the following order of reactivity: glycerol > 1,2-ethanediol > 1,2-propanediol > methanol > ethanol > 2-propanol > *tert*-butanol [178]. Bahruji et al. also reported a similar effect on alcoholic substrates (methanol, ethanol, 2-propanol, 1-propanol, 1-butanol and *tert*-butanol) [171]. Regarding selectivity, it is known that methanol [252] and glycerol [162] afford a complete conversion to CO_2 (mineralisation), while ethanol gives acetaldehyde as the main co-product [168], suggesting a key role of hydroxyl moiety in activation of C-C bond cleavage. It is also known that side pathways yield alkanes from the alkyl chain of alcohols [171], thus lowering hydrogen yield. It is worth noting that these alcohols can be obtained from biomass through chemical [253–255] or biochemical [256] processes, while glycerol is an abundant by-product of the biodiesel industry [257]. Other organic compounds have been also used, such as carboxylic acids and aldehydes, since they constitute bio-oil [258] and wastewater [259]. Wu et al. compared formaldehyde and formic acid, recognised as intermediates in methanol PR, with methanol itself, and found an increase in reactivity as follows: methanol < formaldehyde < formic acid [240]. Likewise, acetic acid was found to be more active than acetaldehyde, while formic acid has showed higher hydrogen yield [252], thus confirming higher reactivity of carboxylic acids and lower reactivity for compounds with longer alkyl chains. Carbohydrates have been extensively used in PR reactions too and are of particular interest as the main components of biomass [260]. Kawai and Sakata firstly reported the use of these compounds in photocatalytic hydrogen evolution, observing a H_2/CO_2 ratio close to stoichiometric value, meaning complete mineralisation of sugar occurred, and a decrease in reactivity moving from simple sugars to polysaccharides [159]. Kondarides et al. studied the reactivity for simple sugars (lactose, cellobiose, maltose), and like Kawai and Sakata, they observed a decrease in hydrogen evolution for starch and cellulose due to their more complex structure [261]. Further study by Caravaca et al. assessed that the size of cellulose also plays a significant role, and moving toward a real lignocellulosic substrate, observed lower yield in hydrogen, although it was higher than pure water [221]. Finally, Speltini et al. have reported some interesting results on waste PR, in particular on olive mill wastewater (OMW) [220] and swine sewage [262], although no complete conversion to CO_2 was observed. PR reaction has also been carried out in a pilot plant using wastewater as substrate and yielding hydrogen, although no complete mineralisation to CO_2 was observed in this case [241].

Another important parameter is reagent concentration. Langmuir's equation has often been observed to fit experimental data on PR reactions in the liquid phase with different substrate and photocatalysts [167,191,263]:

$$r_{H_2} = \frac{k_{H_2} K C_0}{1 + K C_0} \tag{11}$$

where r_{H_2} is the reaction rate, C_0 is the initial substrate concentration, k_{H_2} is the rate constant for hydrogen evolution and K is the adsorption constant. This means that the phenomenon is controlled by substrate adsorption on the catalyst's surface [167]. It has been observed that the addition of little amounts of a hole scavenger (substrate) can increase hydrogen evolution compared to pure water [162], making this process suitable for simultaneous pollutant removal and hydrogen production from very diluted aqueous medium. As the concentration of hole scavenger increased, the hydrogen production was improved too, in both liquid [264] and gas phase [168] systems. Nevertheless, besides a certain upper water-substrate ratio, a decrease in activity or a constant value has been observed in both gas [174] and liquid phase [191,262] conditions, meaning that water becomes the limiting reagent. Moreover, Chiarello et al. suggested that water plays a key role in gas phase conditions, not only as oxidant but also as a proton conductor, allowing a facile transfer from oxidation to reduction sites [166].

Effect on the activity aside, the water-substrate ratio also affects selectivity improving, for higher ratios, complete conversion to CO_2 and reduction of side-products [174].

In the liquid phase, medium acidity and catalyst concentration also have a significant role. The effect of pH is strongly substrate-dependent: methanol [240], acetic acid [172] and cellulose [265] PR on TiO_2 was favoured at neutral pH; OMW, a phenolic-rich mixture, gave better results in acidic media [220] while ethanol [264], glycerol [163], glucose [167] and sewage [262] showed best performances in alkaline solutions. The acidity also plays a crucial role in selectivity. Sakata et al. observed a remarkable decrease in methane formation due to side reaction, in acetic acid PR at higher pH, despite the lower hydrogen yield [172]. As observed by Simon et al., using photoluminescence and transient absorption spectroscopy, alkali-enhanced activity on ethanol PR is due to improved formation of hydroxyl radicals from hydroxyl ion-rich medium, that boost organics decomposition [266]. Finally, one should keep in mind that pH also affects substrate adsorption on catalyst's surface [191,220], catalyst's particle dispersion [240] and pH-dependence on CB and VB [172,266].

Concerning the concentration of catalyst in the suspension reaction medium, it is known that too low an amount of catalyst hinders the activity while too much powder in suspension reduces light penetration [162,262].

3.4. Photoreactors Design

Hence, we want to consider reactor configurations, which is hardly reported and reviewed for PR. Liquid phase reactions are usually carried out in slurry-type reactors, in which the powdered photocatalyst is suspended in the aqueous medium, allowing a good irradiation pattern of the catalyst. The major drawback of this configuration is the catalyst recovery, as experienced in water photoremediation. Immobilisation on a solid support avoids complex separation procedures, though it lowers catalytic activity due to mass-transfer limitations [267]. Concerning gas phase reactions, several different reactor configurations have been reported, such as packed bed [244], plate thin-film [170] and coated honeycomb [175], although no direct comparison among them has been done. It is worth observing that reactor design, as reported in Section 2.2, has a crucial role in photocatalysis, since as we recently report for CO_2 photoreduction, a proper irradiation pattern creates higher productivity with lower amounts of catalyst [74]. Nonetheless, there is plenty of work that can be done on PR reactors' design.

Eventually, the purification of hydrogen in gaseous streams from CO_2 and other by-products should be addressed as issues, in particular, for scaling-up this technology. This problem is actually handled by traditional hydrogen production processes (e.g., methane steam reforming, MSR) [268]. CO_2 removal, the sole H_2 co-product in stoichiometric PR reaction, can be gained by absorption in liquid alkaline solution, as in post-combustion CO_2 capture technologies [269]. The resultant CO_2-rich solution can be used for CO_2 photoreduction in the liquid phase as previously shown in Section 2.2; the combination of these two processes should fulfil both H_2 purification (from CO_2) and avoids CO_2 emission into the atmosphere, while maintaining photocatalysis advantages of mild conditions and solar light utilization. Nonetheless, up until now, none of these processes have been coupled to a PR reaction rig in both gas and liquid phase medium equipment. This additional knowledge can be useful for deeper study on reactor design, for scaling-up PR technology.

In conclusion, the choice of reaction conditions has a crucial impact (Table 5) on process energy efficiency and on enhancing both activity and selectivity. Currently a lack of knowledge about the effect of some parameters such as light irradiance and reactor configuration, as well as no reported works on H_2 purification directly from gaseous PR streams, are critical issues, particularly for scaling-up PR processes and light utilisation efficiency assessment. Moreover, the incomplete conversion to CO_2, i.e., the selectivity of the process, is a crucial issue, since it reduces hydrogen yields, requiring further processing steps in order to "clean" the effluents. This additional knowledge could be useful for evaluating the industrial reliability of this technology as a cheap H_2 source, particularly if one wants to compare PR with other available H_2 production processes.

Table 5. Summary of features to consider on PR reaction improvement.

Issue	Approach	Aim
Light utilisation efficiency	Photon energy close to photocatalyst's bandgap	Reduced photon energy losses
	Low light intensity	Increased AQY (photon utilization)
	Reactor design	Good irradiation pattern of the photocatalyst
Activity enhancement	Increased temperature	Improved product desorption
	Substrate chemical structure	Increased reactivity by increasing the number of hydroxyl moiety
	Increased substrate concentration	Avoiding limiting reactants issues
	pH (substrate-dependent)	Improved decomposition in radical-rich medium (alkaline) or improved substrate adsorption
Selectivity enhancement	Substrate chemical structure	Decrease alkane formation by side reaction by shorter alkyl chains moiety
	Increased water concentration	Improved mineralization by higher water content
	pH (substrate-dependent)	Improved mineralization by enhanced radical formation in alkaline medium

4. Conclusions

CO_2 photoreduction and biomass PR are very challenging processes that could withstand the transition from Anthropocene to Sustainocene, as cited in the introduction. The main advantage of photocatalysis is the direct use of sunlight, a very abundant and cheap primary energy source. Nonetheless, several issues hinder the application on an industrial scale; through this review the main concerns were described. It is clear that upgrading photocatalysis processes is a comprehensive challenge that requires a multidisciplinary approach. Reaction conditions are usually less investigated than photocatalyst formulation, but significantly affect the activity enhancement and further scale-up of these processes. Finally, reactor design is surely a key issue in scaling-up, since both mass-transfer and light-transfer phenomena heavily affect overall efficiency of the process. Though further work is needed, huge efforts have been made on improving photocatalysts, whilst process conditions and reactor design still need to be implemented to achieve promising results, particularly for PR. Thus, there is plenty of work that should be done to improve knowledge and applicability of photocatalysis to solar fuels production.

Author Contributions: All authors equally contributed to the preparation of this manuscript.

Funding: This research and the APC was founded by MIUR (project PRIN 2015 "Heterogeneous Robust Catalysts to Upgrade Low value biomass Streams"), protocol number: 20153T4REF_006

Acknowledgments: Financial support of MIUR (project PRIN 2015 "Heterogeneous Robust Catalysts to Upgrade Low value biomass Streams") is gratefully acknowledged.

Conflicts of Interest: The authors declare no conflict of interest.

References

1. Demibras, A. Potential applications of renewable energy sources, biomass combustion problems in boiler power systems and combustion related environmental issues. *Prog. Energy Combust. Sci.* **2010**, *31*, 171–192.
2. Murphy, D.J.; Hall, C.A.S. Year in review—EROI or energy return on (energy) invested. *Ann. N. Y. Acad. Sci.* **2010**, *1185*, 102–118. [CrossRef] [PubMed]
3. Heede, R.; Oreskes, N. Potential emissions of CO_2 and methane from proved reserves of fossil fuels: An alternative analysis. *Glob. Environ. Chang.* **2016**, *36*, 12–20. [CrossRef]
4. Shaffiee, S.; Topal, E. When will fossil fuel reserves be diminished? *Energy Policy* **2009**, *37*, 181–190. [CrossRef]
5. Scotchman, I.C. Shale gas and fracking: Exploration for unconventional hydrocarbons. *Proc. Geol. Assoc.* **2016**, *127*, 535–551. [CrossRef]
6. Centner, T.J. Observations on risks, the social sciences, and unconventional hydrocarbons. *Energy Res. Soc. Sci.* **2016**, *20*, 1–7. [CrossRef]

7. World Commission on Environment and Development. *Our Common Future*, 1st ed.; Oxford University Press: Oxford, UK, 1987; ISBN 019282080X.
8. Clauser, C.; Ewert, M. The renewables cost challenge: Levelized cost of geothermal electric energy compared to other sources of primary energy—Review and case study. *Renew. Sustain. Energy Rev.* **2018**, *82*, 3683–3693. [CrossRef]
9. Gaffney, S.G.; Marley, N.A. The impacts of combustion emissions on air quality and climate—From coal to biofuels and beyond. *Atmos. Environ.* **2009**, *43*, 23–26. [CrossRef]
10. Garrabrants, A.C.; Kosson, D.S.; DeLapp, R.; van der Sloot, H.A. Effect of coal combustion fly ash use in concrete on the mass transport release of constituents of potential concern. *Chemosphere* **2014**, *103*, 131–139. [CrossRef] [PubMed]
11. Peters, G.P.; Hertwich, E.G. Post-Kyoto greenhouse gas inventories: Production versus consumption. *Clim. Chang.* **2008**, *86*, 51–66. [CrossRef]
12. Data from Global Monitory Division of US National Oceanic and Atmospheric Administration. Available online: https://www.esrl.noaa.gov/gmd/trends/monthly.html (accessed on 8 February 2018).
13. Benhal, E.; Zahedi, G.; Shamsaei, E.; Bahadori, A. Global strategies and potentials to curb CO_2 emissions in cement industry. *J. Clean. Prod.* **2013**, *51*, 142–161. [CrossRef]
14. Figueres, C.; Schellnhuber, H.J.; Rockström, G.W.J.; Hobley, A.; Rahmstorf, S. Three years to safeguard our climate. *Nature* **2017**, *546*, 593–595. [CrossRef] [PubMed]
15. Crutzen, P.J. Geology of mankind. *Nature* **2002**, *415*, 23. [CrossRef] [PubMed]
16. Kyoto Protocol. Available online: http://www.unfccc.int (accessed on 10 February 2018).
17. United Nations Framework Convention on Climate Change (UNFCCC). Adoption of the Paris Agreement. In Proceedings of the 21st Conference of the Parties, Paris, France, 30 November–11 December 2015.
18. Arawaka, H.; Aresta, M.; Armor, J.N.; Barteau, M.A.; Beckman, E.J.; Bell, A.T.; Bercaw, J.E.; Creutz, C.; Dinjus, E.; Dixon, D.A.; et al. Catalysis Research of Relevance to Carbon Management: Progress, Challenges, and Opportunities. *Chem. Rev.* **2001**, *101*, 953–996. [CrossRef]
19. McGlade, C.; Ekins, P. The geographical distribution of fossil fuels unused when limiting global warming to 2 °C. *Nature* **2015**, *517*, 187–190. [CrossRef] [PubMed]
20. MacFarlane, D.R.; Zhang, X.; Kar, M. Measure and control: Molecular management is a key to the Sustainocene! *Green Chem.* **2016**, *18*, 5689–5692. [CrossRef]
21. Graves, C.; Ebbesen, S.D.; Morgensen, M.; Lackner, K.S. Sustainable hydrocarbon fuels by recycling CO_2 and H_2O with renewable or nuclear energy. *Renew. Sustain. Energy Rev.* **2011**, *15*, 1–23. [CrossRef]
22. Schiemer, Q.; Tollefson, J.; Scully, T.; Witze, A.; Morton, O. Energy alternatives: Electricity without carbon. *Nature* **2008**, *454*, 816–823. [CrossRef] [PubMed]
23. Da Silva Veras, T.; Simonato Mozer, T.; da Costa Rubim Messeder dos Santos, D.; da Silva Cesar, A. Hydrogen: Trends, production and characterization of the main process worldwide. *Int. J. Hydrogen Econ.* **2017**, *42*, 2018–2033. [CrossRef]
24. Sharma, S.; Ghoshal, S.K. Hydrogen the future transportation fuel: From production to applications. *Renew. Sustain. Energy Rev.* **2015**, *43*, 1151–1158. [CrossRef]
25. Olah, A.G.; Goeppert, A.; Surya Prakash, G.K. *Beyond Oil and Gas: The Methanol Economy*, 2nd ed.; Wiley-VCH Verlag GmbH & Co. KGaA: Weinheim, Germany, 2009; pp. 156–231, ISBN 978-3-527-32422-4.
26. Antolini, E. Catalysts for direct ethanol fuel cells. *J. Power Sources* **2007**, *170*, 1–12. [CrossRef]
27. Sharaf, O.Z.; Orhan, M.F. An overview of fuel cell technology: Fundamentals and applications. *Renew. Sustain. Energy Rev.* **2014**, *32*, 810–853. [CrossRef]
28. Wang, J. Barriers of scaling-up fuel cells: Cost, durability and reliability. *Energy* **2015**, *80*, 509–521. [CrossRef]
29. Mortensen, P.M.; Grunwaldt, J.-D.; Jensen, P.A.; Knudsen, K.G.; Jensen, A.D. A review of catalytic upgrading of bio-oils to engine fuels. *Appl. Catal. A* **2011**, *407*, 1–19. [CrossRef]
30. Xu, C.; Arancon, R.A.D.; Labidid, J.; Luque, R. Lignin depolymerisation strategies: Towards valuable chemicals and fuels. *Chem. Soc. Rev.* **2014**, *43*, 7485–7500. [CrossRef] [PubMed]
31. Yan, C.; Li, R.; Cui, C.; Liu, S.; Qiu, Q.; Ding, Y.; Wu, Y.; Zhang, B. Catalytic hydroprocessing of microalgae-derived biofuels: A review. *Green Chem.* **2016**, *18*, 3684–3699.
32. Serrano-Ruiz, J.C.; Wang, D.; Dumesic, J.A. Catalytic upgrading of levulinic acid to 5-nonanone. *Green Chem.* **2010**, *12*, 574–577. [CrossRef]

33. Armaroli, N.; Balzani, V. *Energy for a Sustainable World*, 1st ed.; Wiley-VCH Verlag GmbH & Co. KGaA: Weinheim, Germany, 2011; pp. 279–289, ISBN 978-3-527-32540-5.
34. Gupta, R.B. Hydrogen Fuel: Production. In *Transport and Storage*, 1st ed.; CRC Press: Boca Raton, FL, USA, 2009; pp. 187–225, ISBN 978-1-4200-4575-8.
35. Nichele, V.; Signoretto, M.; Menegazzo, F.; Gallo, A.; Dal Santo, V.; Cruciani, G.; Cerrato, G. Glycerol steam reforming for hydrogen production: Design of Ni supported catalysts. *Appl. Catal. B* **2012**, *111–112*, 225–232. [CrossRef]
36. Tripodi, A.; Compagnoni, M.; Ramis, G.; Rossetti, I. Process simulation of hydrogen production by steam reforming of diluted bioethanol solutions: Effect of operating parameters on electrical and thermal cogeneration by using fuel cells. *Int. J. Hydrogen Energy* **2017**, *42*, 23776–23783. [CrossRef]
37. Feng, D.; Zhao, Y.; Zhang, Y.; Zhang, Z.; Zhang, L.; Sun, S. In-situ steam reforming of biomass tar over sawdust biochar in mild catalytic temperature. *Biomass Bioenergy* **2017**, *107*, 261–270. [CrossRef]
38. Guan, G.; Kaewpanha, M.; Hao, X.; Abudula, A. Catalytic steam reforming of biomass tar: Prospects and challenges. *Renew. Sustain. Energy Rev.* **2016**, *58*, 450–461. [CrossRef]
39. Iulianelli, A.; Ribeirinha, P.; Mendes, A.; Basile, A. Methanol steam reforming for hydrogen generation via conventional and membrane reactors: A review. *Renew. Sustain. Energy Rev.* **2014**, *29*, 355–368. [CrossRef]
40. Sims, R.E.H.; Mabee, W.; Saddler, J.N.; Taylor, M. An overview of second generation biofuel technologies. *Biores. Technol.* **2010**, *101*, 1570–1580. [CrossRef] [PubMed]
41. Long, H.; Li, X.; Wang, H.; Jia, J. Biomass resources and their bioenergy potential estimation: A review. *Renew. Sustain. Energy Rev.* **2013**, *26*, 344–352. [CrossRef]
42. Li, D.; Li, X.; Gong, J. Catalytic Reforming of Oxygenates: State of the Art and Future Prospects. *Chem. Rev.* **2016**, *116*, 11529–11653. [CrossRef] [PubMed]
43. Haryanto, A.; Fernando, S.; Murali, N.; Adhikari, S. Current Status of Hydrogen Production Techniques by Steam Reforming of Ethanol: A Review. *Energy Fuels* **2005**, *19*, 2098–2106. [CrossRef]
44. Trane, R.; Dahl, S.; Skjøth-Rasmussen, M.S.; Jensen, A.D. Catalytic steam reforming of bio-oil. *Int. J. Hydrogen Energy* **2012**, *37*, 6447–6472. [CrossRef]
45. Holladay, J.D.; Hu, J.; King, D.L.; Wang, Y. An overview of hydrogen production technologies. *Catal. Today* **2009**, *139*, 244–260. [CrossRef]
46. Puga, A.V. Photocatalytic production of hydrogen from biomass-derived feedstocks. *Coord. Chem. Rev.* **2016**, *315*, 1–66. [CrossRef]
47. Kannann, N.; Vakeesan, D. Solar energy for future world: A review. *Renew. Sustain. Energy Rev.* **2016**, *62*, 1092–1105. [CrossRef]
48. Jiang, Z.; Xiao, T.; Kuznetsov, V.; Edwards, P.P. Turning carbon dioxide into fuel. *Philos. Trans. R. Soc. A* **2010**, *368*, 3343–3364. [CrossRef] [PubMed]
49. Wang, W.; Gong, J. Methanation of carbon dioxide: An overview. *Front. Chem. Sci. Eng.* **2011**, *5*, 2–10.
50. Beaumont, S.K.; Alayoglu, S.; Specht, C.; Michalak, W.D.; Pushkarev, V.V.; Guo, J.; Kruse, N.; Somorjai, G.A. Combining in Situ NEXAFS Spectroscopy and CO_2 Methanation Kinetics To Study Pt and Co Nanoparticle Catalysts Reveals Key Insights into the Role of Platinum in Promoted Cobalt Catalysis. *J. Am. Chem. Soc.* **2017**, *136*, 9898–9901. [CrossRef] [PubMed]
51. Younas, M.; Kong, L.L.; Bashir, M.J.K.; Nadeem, H.; Shehzad, A.; Sethupathu, S. Recent Advancements, Fundamental Challenges, and Opportunities in Catalytic Methanation of CO_2. *Energy Fuels* **2016**, *30*, 8815–8831. [CrossRef]
52. Rossetti, I.; Compagnoni, M.; Torli, M. Process simulation and optimisation of H_2 production from ethanol steam reforming and its use in fuel cells. 1. Thermodynamic and kinetic analysis. *Chem. Eng. J.* **2015**, *281*, 1024–1035. [CrossRef]
53. LeValley, T.L.; Richard, A.R.; Fan, M. The progress in water gas shift and steam reforming hydrogen production technologies—A review. *Int. J. Hydrogen Energy* **2014**, *39*, 16983–17000. [CrossRef]
54. Frontera, P.; Macario, A.; Ferraro, M.; Antonucci, P.L. Supported Catalysts for CO_2 Methanation: A Review. *Catalysts* **2017**, *7*, 59. [CrossRef]
55. Wang, W.; Wang, S.; Ma, X.; Gong, J. Recent advances in catalytic hydrogenation of carbon dioxide. *Chem. Soc. Rev.* **2011**, *40*, 3703–3727. [CrossRef] [PubMed]
56. Hermann, J.-M. Heterogeneous photocatalysis: State of the art and present applications. *Top. Catal.* **2005**, *34*, 49–65.

57. Schneider, J.; Matsuoka, M.; Takeuchi, M.; Zhang, J.; Horiuchi, Y.; Anpo, M.; Bahnemann, D.W. Understanding TiO_2 Photocatalysis: Mechanisms and Materials. *Chem. Rev.* **2014**, *114*, 9919–9986. [CrossRef] [PubMed]
58. Nakata, K.; Fujishima, A. TiO_2 photocatalysis: Design and applications. *J. Photochem. Photobiol. C* **2012**, *13*, 169–189. [CrossRef]
59. Jones-Albertus, R.; Feldman, D.; Fu, R.; Horowitz, K.; Woodhouse, M. Technology advances needed for photovol taics toachieve widespread grid price parity. *Prog. Photovolt. Res. Appl.* **2016**, *24*, 1272–1283. [CrossRef]
60. Haegel, N.M.; Margolis, R.; Buonassisi, T.; Feldman, D.; Froitzheim, A.; Garabedian, R.; Green, M.; Glunz, S.; Henning, H.-M.; Holder, B.; et al. Terawatt-scale photovoltaics: Trajectories and Challenges. *Science* **2017**, *356*, 141–143. [CrossRef] [PubMed]
61. Lewis, N.S.; Nocera, D.G. Powering the planet: Chemical challenges in solar energy utilization. *PNAS* **2007**, *103*, 15729–15735. [CrossRef] [PubMed]
62. Inoue, T.; Fujishima, A.; Konishi, S.; Honda, K. Photoelectrocatalytic reduction of carbon dioxide in aqueous suspensions of semiconductor powders. *Nature* **1979**, *277*, 637–638. [CrossRef]
63. Aurian-Blajeni, B.; Halmann, M.; Manassen, J. Photoreduction of carbon dioxide and water into formaldehyde and methanol on semiconductor materials. *Sol. Energy* **1980**, *25*, 165–170. [CrossRef]
64. Anpo, M.; Yamashita, H.; Ichihashi, Y.; Ehara, S. Photocatalytic reduction of CO_2 with H_2O on Ti-MCM-41 and Ti-MCM-48 mesoporous zeolite catalysts. *J. Electroanal. Chem.* **1995**, *396*, 21–26. [CrossRef]
65. Diebold, U. The surface science of titanium dioxide. *Surf. Sci. Rep.* **2003**, *48*, 53–229. [CrossRef]
66. Markovits, A.; Fahmi, A.; Minot, C. A theoretical study of CO_2 adsorption on TiO_2. *J. Mol. Struct.* **1996**, *371*, 219–235. [CrossRef]
67. Michalkiewicz, B.; Majewska, J.; Kądziołka, G.; Bubacz, K.; Mozia, S.; Morawski, A.W. Reduction of CO_2 by adsorption and reaction on surface of TiO_2-nitrogen modified photocatalyst. *J. CO2 Util.* **2014**, *5*, 47–52. [CrossRef]
68. Krischok, S.; Höfft, O.; Kempter, V. The chemisorption of H_2O and CO_2 on TiO_2 surfaces: Studies with MIES and UPS (HeI/II). *Surf. Sci.* **2002**, *507–510*, 67–73. [CrossRef]
69. Tan, L.L.; Ong, W.J.; Chai, S.P.; Mohamed, A.R. Photocatalytic reduction of CO_2 with H_2O over graphene oxide supported oxygen-rich TiO_2 hybrid photocatalyst under visible light irradiation: Process and kinetic studies. *Chem. Eng. J.* **2017**, *308*, 248–255. [CrossRef]
70. Henderson, M.A. Structural Sensitivity in the Dissociation of Water on TiO_2 Single-Crystal Surfaces. *Langmuir* **1996**, *12*, 5093–5098. [CrossRef]
71. Ketteler, G.; Yamamoto, S.; Bluhm, H.; Andersson, K.; Starr, D.E.; Ogletree, D.F.; Ogasawara, H.; Nilsson, A.; Salmeron, M. The Nature of Water Nucleation Sites on TiO_2(110) Surfaces Revealed by Ambient Pressure X-ray Photoelectron Spectroscopy. *J. Phys. Chem. C* **2007**, *111*, 8278–8282. [CrossRef]
72. Levchenko, A.A.; Li, G.; Boerio-Goates, J.; Woodfield, B.F.; Navrotsky, A. TiO_2 Stability Landscape: Polymorphism, Surface Energy, and Bound Water Energetics. *Chem. Mater.* **2006**, *18*, 6324–6332. [CrossRef]
73. He, H.Y.; Zapol, P.; Curtiss, L.A. Computational screening of dopants for photocatalytic two-electron reduction of CO_2 on anatase (101) surfaces. *Energy Environ. Sci.* **2012**, *5*, 6196–6205. [CrossRef]
74. Olivo, A.; Ghedini, E.; Pascalicchio, P.; Manzoli, M.; Cruciani, G.; Signoretto, M. Sustainable Carbon Dioxide Photoreduction by a Cooperative Effect of Reactor Design and Titania Metal Promotion. *Catalysts* **2018**, *8*, 41. [CrossRef]
75. Jönsson, B.; Karlström, G.; Wennerström, H.; Forsén, S.; Ross, B.; Almlöf, J. Ab initio molecular orbital calculations on the water-carbon dioxide system. Reaction pathway for water + carbon dioxide carbonic acid. *J. Am. Chem. Soc.* **1977**, *99*, 4628–4632. [CrossRef]
76. Nguyen, M.T.; Ha, T.-K. A theoretical study of the formation of carbonic acid from the hydration of carbon dioxide: A case of active solvent catalysis. *J. Am. Chem. Soc.* **1984**, *106*, 599–602. [CrossRef]
77. Merz, K.M., Jr. Gas-phase and solution-phase potential energy surfaces for carbon dioxide + n-water (n = 1,2). *J. Am. Chem. Soc.* **1990**, *112*, 7973–7980. [CrossRef]
78. Sakthivel, S.; Hidalgo, M.C.; Bahnemann, D.W.; Geissen, S.U.; Murugesan, V.; Vogelpohl, A. A fine route to tune the photocatalytic activity of TiO_2. *Appl. Catal. B Environ.* **2006**, *63*, 31–40. [CrossRef]
79. Malato, S.; Blanco, J.; Vidal, A.; Alarcòn, D.; Maldonado, M.I.; Càceres, J.; Gernjak, W. Applied studies in solar photocatalytic detoxification: An overview. *Sol. Energy* **2003**, *75*, 329–336. [CrossRef]

80. Varghese, O.K.; Paulose, M.; LaTempa, T.J.; Grimes, C. High-Rate Solar Photocatalytic Conversion of CO_2 and Water Vapor to Hydrocarbon Fuels. *Nano Lett.* **2009**, *9*, 731–737. [CrossRef] [PubMed]
81. Wu, J.C.S.; Lin, H.M.; Lai, C.L. Photo reduction of CO_2 to methanol using optical-fiber photoreactor. *Appl. Catal. A Gen.* **2005**, *296*, 194–200. [CrossRef]
82. Ikeue, K.; Yamashita, H.; Anpo, M. Photocatalytic Reduction of CO_2 with H_2O on Ti−β Zeolite Photocatalysts: Effect of the Hydrophobic and Hydrophilic Properties. *J. Phys. Chem. B* **2001**, *105*, 8350–8355. [CrossRef]
83. Vijayan, B.; Dimitrijevic, N.M.; Rajh, T.; Gray, K. Effect of Calcination Temperature on the Photocatalytic Reduction and Oxidation Processes of Hydrothermally Synthesized Titania Nanotubes. *J. Phys. Chem. C* **2010**, *114*, 12994–13002. [CrossRef]
84. Woolerton, T.W.; Sheard, S.; Reisner, E.; Pierce, E.; Ragsdale, S.W.; Armstrong, F.A. Efficient and Clean Photoreduction of CO_2 to CO by Enzyme-Modified TiO_2 Nanoparticles Using Visible Light. *J. Am. Chem. Soc.* **2010**, *132*, 2132–2133. [CrossRef] [PubMed]
85. Tahir, M.; Tahir, B.; Amin, N. Synergistic effect in plasmonic Au/Ag alloy NPs co-coated TiO_2 NWs toward visible-light enhanced CO_2 photoreduction to fuels. *Appl. Catal. B Environ.* **2017**, *204*, 548–560. [CrossRef]
86. Olivo, A.; Trevisan, V.; Ghedini, E.; Pinna, F.; Bianchi, C.L.; Naldoni, A.; Cruciani, G.; Signoretto, M. CO_2 photoreduction with water: Catalyst and process investigation. *J. CO2 Util.* **2015**, *12*, 86–94. [CrossRef]
87. Rossetti, I.; Villa, A.; Compagnoni, M.; Prati, L.; Ramis, G.; Pirola, C.; Bianchi, C.L. CO_2 photoconversion to fuels under high pressure: Effect of TiO_2 phase and of unconventional reaction conditions. *Catal. Sci. Technol.* **2015**, *5*, 4481–4487. [CrossRef]
88. Karamian, E.; Sharifnia, S. On the general mechanism of photocatalytic reduction of CO_2. *J. CO2 Util.* **2016**, *16*, 194–203. [CrossRef]
89. Liu, L.; Li, Y. Understanding the Reaction Mechanism of Photocatalytic Reduction of CO_2 with H_2O on TiO_2-Based Photocatalysts: A Review. *Aerosol Air Qual. Res.* **2014**, *14*, 453–569. [CrossRef]
90. Hermann, J.M. Heterogeneous photocatalysis: Fundamentals and applications to the removal of various types of aqueous pollutants. *Catal. Today* **1999**, *53*, 115–129. [CrossRef]
91. Rasko, J.; Solymosi, F. Infrared Spectroscopic Study of the Photoinduced Activation of CO_2 on TiO_2 and Rh/TiO_2 Catalysts. *J. Phys. Chem.* **1994**, *98*, 7147–7152. [CrossRef]
92. Li, K.; An, X.; Park, K.H.; Khraisheh, M.; Tang, J. A critical review of CO_2 photoconversion: Catalysts and reactors. *Catal. Today* **2014**, *224*, 3–12. [CrossRef]
93. Singh, V.; Castellanos Beltran, I.J.; Casamada Ribot, J.; Nagpal, P. Photocatalysis Deconstructed: Design of a New Selective Catalyst for Artificial Photosynthesis. *Nano Lett.* **2014**, *14*, 597–603. [CrossRef] [PubMed]
94. Olivo, A.; Ghedini, E.; Signoretto, M.; Compagnoni, M.; Rossetti, I. Liquid vs. Gas Phase CO_2 Photoreduction Process: Which Is the Effect of the Reaction Medium? *Energies* **2017**, *10*, 1394. [CrossRef]
95. Handoko, A.D.; Li, K.; Tang, J. Recent progress in artificial photosynthesis: CO_2 photoreduction to valuable chemicals in a heterogeneous system. *Curr. Opin. Chem. Eng.* **2013**, *2*, 200–206. [CrossRef]
96. Wang, W.-N.; An, W.-J.; Ramalingam, B.; Mukherjee, S.; Niedzwiedzki, D.M.; Gangopadhyay, S.; Biswas, P. Size and Structure Matter: Enhanced CO_2 Photoreduction Efficiency by Size-Resolved Ultrafine Pt Nanoparticles on TiO_2 Single Crystals. *J. Am. Chem. Soc.* **2012**, *134*, 11276–11281. [CrossRef] [PubMed]
97. Dimitrijevic, N.M.; Vijayan, B.K.; Poluektov, O.G.; Raijh, T.; Gray, K.A.; He, H.; Zapol, P. Role of Water and Carbonates in Photocatalytic Transformation of CO_2 to CH_4 on Titania. *J. Am. Chem. Soc.* **2011**, *133*, 3964–3971. [CrossRef] [PubMed]
98. Tanaka, T.; Kohno, Y.; Yoshida, S. Photoreduction of carbon dioxide by hydrogen and methane. *Res. Chem. Intermed.* **2000**, *26*, 93–101. [CrossRef]
99. Teramura, K.; Tanaka, T.; Ishikawa, H.; Kohno, Y.; Funabiki, T. Photocatalytic Reduction of CO_2 to CO in the Presence of H_2 or CH_4 as a Reductant over MgO. *J. Phys. Chem. B* **2004**, *108*, 346–354. [CrossRef]
100. Baran, T.; Wojtyła, S.; Dibenedetto, A.; Aresta, M.; Macyk, W. Zinc sulfide functionalized with ruthenium nanoparticles for photocatalytic reduction of CO_2. *Appl. Catal. B Environ.* **2015**, *178*, 170–176. [CrossRef]
101. Kočí, K.; Obalová, L.; Matějová, L.; Plachá, D.; Lacný, Z.; Jirkovský, J.; Šolková, O. Effect of TiO_2 particle size on the photocatalytic reduction of CO_2. *Appl. Catal. B Environ.* **2009**, *89*, 494–502. [CrossRef]
102. Galli, F.; Compagnoni, M.; Vitali, D.; Pirola, C.; Bianchi, C.L.; Villa, A.; Prati, L.; Rossetti, I. CO_2 photoreduction at high pressure to both gas and liquid products over titanium dioxide. *Appl. Catal. B Environ.* **2017**, *200*, 386–391. [CrossRef]

103. Ola, O.; Maroto-Valer, M. Role of catalyst carriers in CO_2 photoreduction over nanocrystalline nickel loaded TiO_2-based photocatalysts. *J. Catal.* **2014**, *309*, 300–308. [CrossRef]
104. Marszewski, M.; Cao, S.; Yu, L.; Jaronec, M. Semiconductor-based photocatalytic CO_2 conversion. *Mater. Horiz.* **2015**, *2*, 261–276. [CrossRef]
105. Dimitrijevic, N.M.; Shkrob, I.A.; Gosztola, D.J.; Raji, T. Dynamics of Interfacial Charge Transfer to Formic Acid, Formaldehyde, and Methanol on the Surface of TiO_2 Nanoparticles and Its Role in Methane Production. *J. Phys. Chem. C* **2012**, *116*, 878–885. [CrossRef]
106. Clarizia, L.; Di Somma, I.; Onotri, L.; Andreozzi, R.; Marotta, R. Kinetic modeling of hydrogen generation over nano-$Cu_{(s)}/TiO_2$ catalyst through photoreforming of alcohols. *Catal. Today* **2017**, *281*, 117–123. [CrossRef]
107. Matějová, L.; Šihor, M.; Lang, J.; Troppová, I.; Ambrožová, N.; Reli, M.; Brunátová, T.; Čapek, L.; Kotarba, A.; Kočí, K. Investigation of low Ce amount doped-TiO_2 prepared by using pressurized fluids in photocatalytic N_2O decomposition and CO_2 reduction. *J. Sol-Gel Sci. Technol.* **2017**, *84*, 158–168. [CrossRef]
108. Tan, S.; Zou, L.; Hu, E. Photocatalytic reduction of carbon dioxide into gaseous hydrocarbon using TiO_2 pellets. *Catal. Today* **2006**, *115*, 269–273. [CrossRef]
109. Bessekhouad, Y.; Robert, D.; Weber, J.-V. Photocatalytic activity of Cu_2O/TiO_2,Bi_2O_3/TiO_2 and $ZnMn_2O_4/TiO_2$ heterojunctions. *Catal. Today* **2005**, *101*, 315–321. [CrossRef]
110. Kaneco, S.; Shimizu, Y.; Ohta, K.; Mizuno, T. Photocatalytic reduction of high pressure carbon dioxide using TiO_2 powders with a positive hole scavenger. *J. Photochem. Photobiol. A Chem.* **1998**, *115*, 223. [CrossRef]
111. Lee, W.H.; Liao, C.H.; Tsai, M.F.; Huang, C.W.; Wu, J.C.S. A novel twin reactor for CO_2 photoreduction to mimic artificial photosynthesis. *Appl. Catal. B Environ.* **2013**, *132–133*, 445–451. [CrossRef]
112. Truong, Q.D.; Le, T.H.; Liu, J.Y.; Chung, C.C.; Ling, Y.C. Synthesis of TiO_2 nanoparticles using novel titanium oxalate complex towards visible light-driven photocatalytic reduction of CO_2 to CH_3OH. *Appl. Catal. A Gen.* **2012**, *437–438*, 28–35. [CrossRef]
113. Liu, L.; Gao, F.; Zhao, H.; Li, Y. Tailoring Cu valence and oxygen vacancy in Cu/TiO_2 catalysts for enhanced CO_2 photoreduction efficiency. *Appl. Catal. B Environ.* **2013**, *134–135*, 349–358. [CrossRef]
114. Tahir, M.; Amin, N. Photocatalytic CO_2 reduction with H_2O vapors using montmorillonite/TiO_2 supported microchannel monolith photoreactor. *Chem. Eng. J.* **2013**, *230*, 314–327. [CrossRef]
115. Lo, C.C.; Hung, C.H.; Yuan, C.S.; Hung, Y.L. Parameter Effects and Reaction Pathways of Photoreduction of CO_2 over TiO_2/SO_4^{2-} Photocatalyst. *Chin. J. Catal.* **2007**, *28*, 528–534. [CrossRef]
116. Das, S.; Wan Daud, W.M.A. A review on advances in photocatalysts towards CO_2 conversion. *RCS Adv.* **2014**, *4*, 20856–20893. [CrossRef]
117. Tahir, M.; Amin, N. Recycling of carbon dioxide to renewable fuels by photocatalysis: Prospects and challenges. *Renew. Sustain. Energy Rev.* **2013**, *25*, 560–579. [CrossRef]
118. Liu, G.; Hoivik, N.; Wang, K.; Jakobsen, H. Engineering TiO_2 nanomaterials for CO_2 conversion/solar fuels. *Sol. Energy Mater. Sol Cells* **2012**, *105*, 53–68. [CrossRef]
119. Cook, R.L.; MacDuff, R.C.; Sammells, A.F. Photoelectrochemical Carbon Dioxide Reduction to Hydrocarbons at Ambient Temperature and Pressure. *J. Electrochem. Soc.* **1988**, *135*, 3069–3070. [CrossRef]
120. Dey, G.; Belapurkar, A.; Kishore, K. Photo-catalytic reduction of carbon dioxide to methane using TiO_2 as suspension in water. *J. Photochem. Photobiol. A* **2004**, *163*, 503–508. [CrossRef]
121. Kočí, K.; Obalová, L.; Lacný, Z. Photocatalytic reduction of CO_2 over TiO_2 based catalysts. *Chem. Pap.* **2008**, *62*, 1–9. [CrossRef]
122. Ichikawa, S.; Doi, R. Hydrogen production from water and conversion of carbon dioxide to useful chemicals by room temperature photoelectrocatalysis. *Catal. Today* **1995**, *27*, 271–277. [CrossRef]
123. Hasan, R.; Hamid, S.B.A.; Basirun, W.J.; Chowdhury, Z.Z.; Kandjani, A.E.; Bhargava, S.K. Ga doped RGO–TiO_2 composite on an ITO surface electrode for investigation of photoelectrocatalytic activity under visible light irradiation. *New J. Chem.* **2015**, *39*, 369–376. [CrossRef]
124. Gering, K.L. Photoreactor with Self-Contained Photocatalyst Recapture. U.S. Patent US6827911 B1, 2004.
125. Funken, K.H.; Sattler, C.; Ortner, J. Lde Oliveira, Solar Photoreactor. U.S. Patent US6633042 B1, 2017.
126. Perry, R.H.; Green, D.W.; Maloney, J.O. *Perry's Chemical Engineers' Handbook*, 7th ed.; McGraw-Hill: New York, NY, USA, 1999; pp. 2-241–2-243, ISBN 0-07-049841-5.

127. Anpo, M.; Yamashita, H.; Ikeue, K.; Fujii, Y.; Zhang, S.G.; Ichihashi, Y.; Park, D.R.; Suzuki, Y.; Koyano, K.; Tatsumi, T. Selective formation of CH_3OH in the photocatalytic reduction of CO_2 with H_2O on titanium oxides highly dispersed within zeolites and mesoporous molecular sieves. *Catal. Today* **1998**, *44*, 327–331. [CrossRef]
128. Richardson, P.L.; Perdigoto, M.L.N.; Wang, W.; Lopes, R.J.G. Heterogeneous photo-enhanced conversion of carbon dioxide to formic acid with copper- and gallium-doped titania nanocomposites. *Appl. Catal. B Environ.* **2013**, *132–133*, 408–415. [CrossRef]
129. Ola, O.; Maroto-Valer, M. Review of material design and reactor engineering on TiO_2 photocatalysis for CO_2 reduction. *J. Photochem. Photobiol. C* **2015**, *24*, 16–42. [CrossRef]
130. Mizuno, T.; Kengi, A.; Kiyohisa, O.; Akira, S. Effect of CO_2 pressure on photocatalytic reduction of CO_2 using TiO_2 in aqueous solutions. *J. Photochem. Photobiol. A* **1996**, *98*, 87–90. [CrossRef]
131. Li, X.; Chen, J.; Li, H.; Li, J.; Xu, Y.; Liu, Y.; Zhou, J. Photoreduction of CO_2 to methanol over Bi_2S_3/CdS photocatalyst under visible light irradiation. *J. Nat. Gas Chem.* **2011**, *20*, 413–417. [CrossRef]
132. Truong, Q.D.; Liu, J.-L.; Chung, C.-C.; Ling, Y.-C. Photocatalytic reduction of CO_2 on $FeTiO_3/TiO_2$ photocatalyst. *Catal. Commun.* **2012**, *19*, 85–89. [CrossRef]
133. Halmann, M. Photoelectrochemical reduction of aqueous carbon dioxide on p-type gallium phosphide in liquid junction solar cells. *Nature* **1978**, *275*, 115–116. [CrossRef]
134. Fujiwara, H.; Hosokawa, H.; Murakoshi, K.; Wada, Y.; Yanagida, S.; Okada, T.; Yanagida, S. Effect of Surface Structures on Photocatalytic CO_2 Reduction Using Quantized CdS Nanocrystallites. *J. Phys. Chem. B* **1997**, *101*, 8270–8278. [CrossRef]
135. Qin, S.; Xin, F.; Liu, Y.; Yin, X.; Ma, W. Photocatalytic reduction of CO_2 in methanol to methyl formate over CuO–TiO_2 composite catalysts. *J. Colloid Interface Sci.* **2011**, *356*, 257–261. [CrossRef] [PubMed]
136. Liu, B.-J.; Torimoto, T.; Yoneyama, H. Photocatalytic reduction of CO_2 using surface-modified CdS photocatalysts in organic solvents. *J. Photochem. Photobiol. A* **1998**, *113*, 93–97. [CrossRef]
137. Compagnoni, M.; Ramis, G.; Freyria, F.S.; Armandi, M.; Bonelli, B.; Rossetti, I. Innovative photoreactors for unconventional photocatalytic processes: The photoreduction of CO_2 and the photo-oxidation of ammonia. *Rend. Lincei* **2017**, *28* (Suppl. 1), 151–158. [CrossRef]
138. Kaneco, S.; Kurimoto, H.; Ohta, K.; Mizuno, T.; Saji, A. Photocatalytic reduction of CO_2 using TiO_2 powders in liquid CO_2 medium. *J. Photochem. Photobiol. A* **1997**, *109*, 59–63. [CrossRef]
139. Bideau-Mehu, A.; Guern, Y.; Abjean, R.; Johannin-Gilles, A. Interferometric determination of the refractive index of carbon dioxide in the ultraviolet region. *Opt. Commun.* **1973**, *9*, 432–434. [CrossRef]
140. Zhang, Q.; Gao, T.; Andino, J.M.; Li, Y. Copper and iodine co-modified TiO_2 nanoparticles for improved activity of CO_2 photoreduction with water vapor. *Appl. Catal. B Environ.* **2012**, *123–124*, 257–267. [CrossRef]
141. Tahir, M.; Amin, N. Photocatalytic reduction of carbon dioxide with water vapors over montmorillonite modified TiO_2 nanocomposites. *Appl. Catal. B Environ.* **2013**, *142–143*, 512–522. [CrossRef]
142. Matějová, L.; Kočí, K.; Reli, M.; Čapek, L.; Hospodková, A.; Peikertová, P.; Matěj, Z.; Obalová, L.; Wach, A.; Kuśtrowski, P. Preparation, characterization and photocatalytic properties of cerium doped TiO_2: On the effect of Ce loading on the photocatalytic reduction of carbon dioxide. *Appl. Catal. B Environ.* **2014**, *152–153*, 172–183. [CrossRef]
143. Bazzo, A.; Urawaka, A. Origin of photocatalytic activity in continuous gas phase CO_2 reduction over Pt/TiO_2. *ChemSusChem* **2013**, *6*, 2095–2102. [CrossRef] [PubMed]
144. Collado, L.; Jana, P.; Sierra, B.; Coronado, J.M.; Pizarro, P.; Serrano, D.P.; de la Peña O'Shea, V.A. Enhancement of hydrocarbon production via artificial photosynthesis due to synergetic effect of Ag supported on TiO_2 and ZnO semiconductors. *Chem. Eng. J.* **2013**, *224*, 128–135. [CrossRef]
145. Tahir, M.; Amin, N. Indium-doped TiO_2 nanoparticles for photocatalytic CO_2 reduction with H_2O vapors to CH_4. *Appl. Catal. B Environ.* **2015**, *162*, 98–109. [CrossRef]
146. Cybula, A.; Klein, M.; Zaleska, A. Methane formation over TiO_2-based photocatalysts: Reaction pathways. *Appl. Catal. B Environ.* **2015**, *164*, 433–442. [CrossRef]
147. Tahir, M.; Amin, N. Advances in visible light responsive titanium oxide-based photocatalysts for CO_2 conversion to hydrocarbon fuels. *Energy Convers. Manag.* **2013**, *76*, 194–214. [CrossRef]
148. Raupp, G.A.; Nico, J.A.; Annagi, S.; Changrani, R.; Annapragada, R. Two-Flux Radiation-Field Model for an Annular Packed-Bed Photocatalytic Oxidation Reactor. *AIChE J.* **2004**, *43*, 792–801. [CrossRef]

149. Kočí, K.; Reli, M.; Kozák, O.; Lacný, Z.; Plachá, D.; Plaus, P.; Obalová, L. Influence of reactor geometry on the yield of CO_2 photocatalytic reduction. *Catal. Today* **2011**, *176*, 212–214. [CrossRef]
150. Wu, J.C.S.; Lin, H.M. Photo reduction of CO_2 to methanol via TiO_2 photocatalyst. *Int. J. Photoenergy* **2005**, *7*, 115–119. [CrossRef]
151. Ola, O.; Maroto-Valer, M. Synthesis, characterization and visible light photocatalytic activity of metal based TiO_2 monoliths for CO_2 reduction. *Chem. Eng. J.* **2016**, *283*, 1244–1253. [CrossRef]
152. Van Gerven, T.; Mul, G.; Moulijn, J.; Stankiewicz, A. A review of intensification of photocatalytic processes. *Chem. Eng. Process.* **2007**, *46*, 781–789. [CrossRef]
153. Howe, R. Recent Developments in Photocatalysis. *Dev. Chem. Eng. Miner. Process.* **1998**, *6*, 55–84. [CrossRef]
154. Pathak, P.; Meziani, M.J.; Li, Y.; Cureton, L.T.; Sun, Y.P. Improving photoreduction of CO_2 with homogeneously dispersed nanoscale TiO_2 catalysts. *Chem. Commun.* **2014**, *10*, 1234–1235. [CrossRef]
155. Hisatomi, T.; Kubota, J.; Domen, K. Recent advances in semiconductors for photocatalytic and photoelectrochemical water splitting. *Chem. Soc. Rev.* **2014**, *43*, 7520–7535. [CrossRef] [PubMed]
156. Ma, Y.; Wang, X.; Jia, Y.; Chen, X.; Han, H.; Li, C. Titanium Dioxide-Based Nanomaterials for Photocatalytic Fuel Generations. *Chem. Rev.* **2014**, *114*, 9987–10043. [CrossRef] [PubMed]
157. Jitputti, J.; Pavasupree, S.; Suzuki, Y.; Yoshikawa, S. Synthesis and photocatalytic activity for water-splitting reaction of nanocrystalline mesoporous titania prepared by hydrothermal method. *J. Solid State Chem.* **2007**, *180*, 1743–1749. [CrossRef]
158. Sun, W.; Zhang, S.; Wang, C.; Liu, Z.; Mao, Z. Effects of Cocatalyst and Calcination Temperature on Photocatalytic Hydrogen Evolution Over $BaTi_4O_9$ Powder Synthesized by the Polymerized Complex Method. *Catal. Lett.* **2008**, *123*, 282–288. [CrossRef]
159. Kawai, T.; Sakata, T. Conversion of carbohydrate into hydrogen fuel by a photocatalytic process. *Nature* **1980**, *286*, 474–476. [CrossRef]
160. Al-Mazroai, L.S.; Bowker, M.; Davies, P.; Dickinson, A.; Greaves, J.; James, D.; Millard, L. The photocatalytic reforming of methanol. *Catal. Today* **2007**, *122*, 46–50. [CrossRef]
161. Romero Ocana, I.; Beltram, A.; Delgado Jaen, J.J.; Adami, G.; Montini, T.; Fornasiero, P. Photocatalytic H_2 production by ethanol photodehydrogenation: Effect of anatase/brookite nanocomposites composition. *Inorg. Chim. Acta* **2015**, *431*, 197–205. [CrossRef]
162. Daskalaki, V.M.; Kondarides, D.I. Efficient production of hydrogen by photo-induced reforming of glycerol at ambient conditions. *Catal. Today* **2009**, *144*, 75–80. [CrossRef]
163. Gaya, U.I.; Abdullah, A.H. Heterogeneous photocatalytic degradation of organic contaminants over titanium dioxide: A review of fundamentals, progress and problems. *J. Photochem. Photobiol. C* **2008**, *9*, 1–12. [CrossRef]
164. Yan, Z.; Wu, H.; Han, A.; Yu, X.; Du, P. Noble metal-free cobalt oxide (CoO_x) nanoparticles loaded on titanium dioxide/cadmium sulfide composite for enhanced photocatalytic hydrogen production from water. *Int. J. Hydrogen Energy* **2014**, *39*, 13353–13360. [CrossRef]
165. Jing, D.; Zhang, Y.; Guo, L. Study on the synthesis of Ni doped mesoporous TiO_2 and its photocatalytic activity for hydrogen evolution in aqueous methanol solution. *Chem. Phys. Lett.* **2005**, *415*, 74–78. [CrossRef]
166. Chiarello, G.L.; Ferri, D.; Selli, E. Effect of the CH_3OH/H_2O ratio on the mechanism of the gas-phase photocatalytic reforming of methanol on noble metal-modified TiO_2. *J. Catal.* **2011**, *280*, 168–177. [CrossRef]
167. Fu, X.; Long, J.; Wang, X.; Leung, D.Y.C.; Ding, Z.; Wu, L.; Zhang, Z.; Li, Z.; Fu, X. Photocatalytic reforming of biomass: A systematic study of hydrogen evolution from glucose solution. *Int. J. Hydrogen Energy* **2008**, *33*, 6484–6941. [CrossRef]
168. Puga, A.V.; Forneli, A.; García, H.; Corma, A. Production of H_2 by Ethanol Photoreforming on Au/TiO_2. *Adv. Funct. Mater.* **2014**, *24*, 241–248. [CrossRef]
169. Bamwenda, G.R.; Tsubota, S.; Nakamura, T.; Haruta, M. Photoassisted hydrogen production from a water-ethanol solution: A comparison of activities of $Au\text{-}TiO_2$ and $Pt\text{-}TiO_2$. *J. Photochem. Photobiol. A* **1995**, *89*, 177–189. [CrossRef]
170. Ampelli, C.; Genovese, C.; Passalacqua, R.; Perathoner, S.; Centi, G. A gas-phase reactor powered by solar energy and ethanol for H_2 production. *Appl. Therm. Eng.* **2014**, *70*, 1270–1275. [CrossRef]
171. Bahruji, H.; Bowker, M.; Davies, P.R.; Al-Mazroai, L.S.; Dickinson, A.; Greaves, J.; James, D.; Millard, L.; Pedrono, F. Sustainable H_2 gas production by photocatalysis. *J. Photochem. Photobiol. A* **2010**, *216*, 115–118. [CrossRef]

172. Sakata, T.; Kawai, T.; Hashimoto, K. Heterogeneous Photocatalytic Reactions of Organic Acids and Water. New Reaction Paths besides the Photo-Kolbe Reaction. *J. Phys. Chem.* **1984**, *88*, 2344–2350. [CrossRef]
173. Hashimoto, K.; Kawai, T.; Sakata, T. Photocatalytic Reactions of Hydrocarbons and Fossil Fuels with Water. Hydrogen Production and Oxidation. *J. Phys. Chem.* **1984**, *88*, 4083–4088. [CrossRef]
174. Chiarello, G.L.; Aguirre, M.H.; Selli, E. Hydrogen production by photocatalytic steam reforming of methanol on noble metal-modified TiO_2. *J. Catal.* **2010**, *273*, 182–190. [CrossRef]
175. Taboada, E.; Angurell, I.; Llorca, J. Dynamic photocatalytic hydrogen production from ethanol–water mixtures in an optical fiber honeycomb reactor loaded with Au/TiO_2. *J. Catal.* **2014**, *309*, 460–467. [CrossRef]
176. Lu, H.; Zhao, J.; Li, L.; Gong, L.; Zheng, J.; Zhang, L.; Wang, Z.; Zhang, J.; Zhu, Z. Selective oxidation of sacrificial ethanol over TiO_2-based photocatalysts during water splitting. *Energy Environ. Sci.* **2011**, *4*, 3384–3388. [CrossRef]
177. Li, J.; Wu, N. Semiconductor-based photocatalysts and photoelectrochemical cells for solar fuel generation: A review. *Catal. Sci. Technol.* **2015**, *5*, 1360–1384. [CrossRef]
178. Al-Azri, Z.H.N.; Chen, W.-T.; Chan, A.; Jovic, V.; Ina, T.; Idriss, H.; Waterhouse, G.I.N. The roles of metal co-catalysts and reaction media in photocatalytic hydrogen production: Performance evaluation of M/TiO_2 photocatalysts (M = Pd, Pt, Au) in different alcohol–water mixtures. *J. Catal.* **2015**, *329*, 353–367. [CrossRef]
179. Chen, X.; Mao, S.S. Titanium Dioxide Nanomaterials: Synthesis, Properties, Modifications, and Applications. *Chem. Rev.* **2007**, *107*, 2891–2959. [CrossRef] [PubMed]
180. Lv, R.; Wang, X.; Lv, W.; Xu, Y.; Ge, Y.; He, H.; Li, G.; Wu, X.; Li, X.; Li, Q. Facile synthesis of ZnO nanorods grown on graphene sheets and its enhanced photocatalytic efficiency. *J. Chem. Technol. Biotechnol.* **2015**, *90*, 550–558. [CrossRef]
181. Barreca, D.; Fornasiero, P.; Gasparotto, A.; Gombac, V.; Maccato, C.; Montini, T.; Tondello, E. The Potential of Supported Cu_2O and CuO Nanosystems in Photocatalytic H_2 Production. *ChemSusChem* **2009**, *2*, 230–233. [CrossRef] [PubMed]
182. Zieliñska, B.; Borowiak-Palen, E.; Kalenczuk, R.J. Photocatalytic hydrogen generation over alkaline-earth titanates in the presence of electron donors. *Int. J. Hydrogen Energy* **2008**, *33*, 1797–1802. [CrossRef]
183. Kato, H.; Asakura, K.; Kudo, A. Highly Efficient Water Splitting into H_2 and O_2 over Lanthanum-Doped $NaTaO_3$ Photocatalysts with High Crystallinity and Surface Nanostructure. *J. Am. Chem. Soc.* **2003**, *125*, 3082–3089. [CrossRef] [PubMed]
184. Zeng, G.-S.; Yu, J.; Zhu, H.-Y.; Liu, H.-L.; Xing, Q.-J.; Bao, S.-K.; He, S.; Zou, J.-P.; Au, C.-T. Controllable synthesis of $InTaO_4$ catalysts of different morphologies using a versatile sol precursor for photocatalytic evolution of H_2. *RSC Adv.* **2015**, *5*, 37603–37609. [CrossRef]
185. Peng, R.; Wu, C.-M.; Baltrusaitis, J.; Dimitrijevic, N.M.; Ranjit, T.R.; Koodali, T. Ultra-stable CdS incorporated Ti-MCM-48 mesoporous materials for efficient photocatalytic decomposition of water under visible light illumination. *Chem. Commun.* **2013**, *49*, 3221–3223. [CrossRef] [PubMed]
186. Luo, Y.; Liu, X.; Tang, X.; Luo, Y.; Zeng, Q.; Deng, X.; Dinga, S.; Sun, Y. Gold nanoparticles embedded in Ta_2O_5/Ta_3N_5 as active visible-light plasmonic photocatalysts for solar hydrogen evolution. *J. Mater. Chem. A* **2014**, *2*, 14927–14939. [CrossRef]
187. Ma, S.S.K.; Maeda, K.; Domen, K. Modification of TaON with ZrO_2 to improve photocatalytic hydrogen evolution activity under visible light: Influence of preparation conditions on activity. *Catal. Sci. Technol.* **2012**, *2*, 818–823. [CrossRef]
188. Lavorato, C.; Primo, A.; Molinari, R.; Garcia, H. N-Doped Graphene Derived from Biomass as a Visible-Light Photocatalyst for Hydrogen Generation from Water/Methanol Mixtures. *Chem. Eur. J.* **2014**, *20*, 187–194. [CrossRef] [PubMed]
189. Yang, S.; Gong, Y.; Zhang, J.; Zhan, L.; Ma, L.; Fang, Z.; Vajtai, R.; Wang, X.; Ajayan, P.M. Exfoliated Graphitic Carbon Nitride Nanosheets as Efficient Catalysts for Hydrogen Evolution Under Visible Light. *Adv. Mater.* **2013**, *25*, 2452–2456. [CrossRef] [PubMed]
190. Jing, D.; Liu, M.; Shi, J.; Tang, W.; Guo, L. Hydrogen production under visible light by photocatalytic reforming of glucose over an oxide solid solution photocatalyst. *Catal. Commun.* **2010**, *12*, 264–267. [CrossRef]
191. Peng, S.; Ding, M.; Yi, T.; Zhan, Z.; Li, Y. Photocatalytic Hydrogen Evolution and Decomposition of Glycerol over $Cd_{0.5}Zn_{0.5}S$ Solid Solution under Visible Light Irradiation. *Environ. Prog. Sustain. Energy* **2016**, *35*, 141–148. [CrossRef]

192. Jitputti, J.; Suzuki, Y.; Yoshikawa, S. Synthesis of TiO_2 nanowires and their photocatalytic activity for hydrogen evolution. *Catal. Commun.* **2008**, *9*, 1265–1271. [CrossRef]
193. Yu, J.; Qi, L.; Jaroniec, M. Hydrogen Production by Photocatalytic Water Splitting over Pt/TiO_2 Nanosheets with Exposed (001) Facets. *J. Phys. Chem. C* **2010**, *114*, 13118–13125. [CrossRef]
194. Cui, X.; Wang, Y.; Jiang, G.; Zhao, Z.; Xu, C.; Wei, Y.; Duan, A.; Liu, J.; Gao, J. A photonic crystal-based CdS–Au–WO_3 heterostructure for efficient visible-light photocatalytic hydrogen and oxygen evolution. *RSC Adv.* **2014**, *4*, 15689–15694. [CrossRef]
195. Carmichael, P.; Hazafy, D.; Bhachu, D.S.; Mills, A.; Darra, J.A.; Parkin, I.P. Atmospheric pressure chemical vapour deposition of boron doped titanium dioxide for photocatalytic water reduction and oxidation. *Phys. Chem. Chem. Phys.* **2013**, *15*, 16788–16794. [CrossRef] [PubMed]
196. Kanade, K.G.; Kale, B.B.; Baeg, J.-O.; Lee, S.M.; Lee, C.W.; Moon, S.-J.; Chang, H. Self-assembled aligned Cu doped ZnO nanoparticles for photocatalytic hydrogen production under visible light irradiation. *Mater. Chem. Phys.* **2007**, *102*, 98–104. [CrossRef]
197. Zhang, S.; Peng, B.; Yang, S.; Fang, Y.; Peng, F. The influence of the electrodeposition potential on the morphology of Cu_2O/TiO_2 nanotube arrays and their visible-light-driven photocatalytic activity for hydrogen evolution. *Int. J. Hydrogen Energy* **2013**, *38*, 13866–13871. [CrossRef]
198. Daskalaki, V.M.; Antoniaudou, M.; Li Puma, G.; Kondarides, D.I.; Lianos, P. Solar Light-Responsive $Pt/CdS/TiO_2$ Photocatalysts for Hydrogen Production and Simultaneous Degradation of Inorganic or Organic Sacrificial Agents in Wastewater. *Environ. Sci. Technol.* **2010**, *44*, 7200–7205. [CrossRef] [PubMed]
199. Xiao, S.; Liu, P.; Zhu, W.; Li, G.; Zhang, D.; Li, H. Copper Nanowires: A Substitute for Noble Metals to Enhance Photocatalytic H_2 Generation. *Nano Lett.* **2015**, *15*, 4853–4858. [CrossRef] [PubMed]
200. Wang, X.; Liu, G.; Lu, G.Q.; Cheng, H.-M. Stable photocatalytic hydrogen evolution from water over ZnO–CdS core–shell nanorods. *Int. J. Hydrogen Energy* **2010**, *35*, 8199–8205. [CrossRef]
201. Kida, T.; Guan, G.; Yamada, N.; Ma, T.; Kimura, K.; Yoshida, A. Hydrogen production fromsewage sludge solubilized in hot-compressed water using photocatalyst under light irradiation. *Int. J. Hydrogen Energy* **2004**, *29*, 269–274. [CrossRef]
202. Tran, P.D.; Batabyal, S.K.; Pramana, S.S.; Barber, J.; Wong, L.H.; Loo, S.C.J. A cuprous oxide–reduced graphene oxide (Cu_2O–rGO) composite photocatalyst for hydrogen generation: Employing rGO as an electron acceptor to enhance the photocatalytic activity and stability of Cu_2O. *Nanoscale* **2012**, *4*, 3875–3878. [CrossRef] [PubMed]
203. Ye, A.; Fan, W.; Zhang, Q.; Deng, W.; Wang, Y. CdS–graphene and CdS–CNT nanocomposites as visible-light photocatalysts for hydrogen evolution and organic dye degradation. *Catal. Sci. Technol.* **2012**, *2*, 969–978. [CrossRef]
204. Yuzawa, H.; Yoshida, T.; Yoshida, H. Gold nanoparticles on titanium oxide effective for photocatalytic hydrogen formation under visible light. *Appl. Catal. B* **2012**, *115–116*, 294–302. [CrossRef]
205. Zhang, S.; Peng, B.; Yang, S.; Wang, H.; Yu, H.; Fang, Y.; Peng, F. Non-noble metal copper nanoparticles-decorated TiO_2 nanotube arrays with plasmon-enhanced photocatalytic hydrogen evolution under visible light. *Int. J. Hydrogen Energy* **2015**, *40*, 303–310. [CrossRef]
206. Fu, X.; Wang, X.; Leung, D.Y.C.; Xue, W.; Ding, Z.; Huang, H.; Fu, X. Photocatalytic reform ing of glucose over La doped alkali tantalate photocatalysts for H_2 production. *Catal. Commun.* **2010**, *12*, 184–187. [CrossRef]
207. Xiang, Q.; Yu, J.; Jaroniec, M. Preparation and Enhanced Visible-Light Photocatalytic H_2-Production Activity of Graphene/C_3N_4 Composites. *J. Phys. Chem. C* **2011**, *115*, 7355–7363. [CrossRef]
208. Bard, A.J. Photoelectrochemistry and heterogeneous photocatalysis at semiconductors. *J. Photochem.* **1979**, *10*, 59–75. [CrossRef]
209. Sasaki, Y.; Nemoto, H.; Saito, K.; Kudo, A. Solar Water Splitting Using Powdered Photocatalysts Driven by Z-Schematic Interparticle Electron Transfer without an Electron Mediator. *J. Phys. Chem. C* **2009**, *113*, 17536–17542. [CrossRef]
210. Zhou, P.; Yu, J.; Jaroniec, M. All-Solid-State Z-Scheme Photocatalytic Systems. *Adv. Mater.* **2014**, *26*, 4920–4935. [CrossRef] [PubMed]
211. Yu, Z.B.; Xie, Y.P.; Liu, G.; Lu, G.Q.; Ma, X.L.; Cheng, H.-M. Self-assembled CdS/Au/ZnO heterostructure induced by surface polar charges for efficient photocatalytic hydrogen evolution. *J. Mater. Chem. A* **2013**, *1*, 2773–2776. [CrossRef]

212. Fu, N.; Jin, Z.; Wu, Y.; Lu, G.; Li, D. Z-Scheme Photocatalytic System Utilizing Separate Reaction Centers by Directional Movement of Electrons. *J. Phys. Chem. C* **2011**, *115*, 8586–8593. [CrossRef]
213. Yu, W.; Chen, J.; Shang, T.; Chen, L.; Gu, L.; Peng, T. Direct Z-scheme g-C_3N_4/WO_3 photocatalyst with atomically defined junction for H_2 production. *Appl. Catal. B* **2017**, *219*, 693–704. [CrossRef]
214. Tanaka, A.; Hashimoto, K.; Kominami, H. Visible-Light-Induced Hydrogen and Oxygen Formation over Pt/Au/WO_3 Photocatalyst Utilizing Two Types of Photoabsorption Due to Surface Plasmon Resonance and Band-Gap Excitation. *J. Am. Chem. Soc.* **2014**, *136*, 586–589. [CrossRef] [PubMed]
215. Chiarello, G.L.; Forni, L.; Selli, E. Photocatalytic hydrogen production by liquid- and gas-phase reforming of CH_3OH over flame-made TiO_2 and Au/TiO_2. *Catal. Today* **2009**, *144*, 69–74. [CrossRef]
216. Yu, J.; Hai, Y.; Jaroniec, M. Photocatalytic hydrogen production over CuO-modified titania. *J. Colloid Interface Sci.* **2011**, *357*, 223–228. [CrossRef] [PubMed]
217. Subramanian, V.; Wolf, E.E.; Kamat, P.V. Catalysis with TiO_2/Gold Nanocomposites. Effect of Metal Particle Size on the Fermi Level Equilibration. *J. Am. Chem. Soc.* **2004**, *126*, 4943–4950. [CrossRef] [PubMed]
218. Ai, G.; Li, H.; Liu, S.; Mo, R.; Zhong, J. Solar Water Splitting by TiO_2/CdS/Co–Pi Nanowire Array Photoanode Enhanced with Co-Pi as Hole Transfer Relay and CdS as Light Absorber. *Adv. Funct. Mater.* **2015**, *25*, 5706–5713. [CrossRef]
219. Bowker, M.; Millard, L.; Greaves, J.; James, D.; Soares, J. Photocatalysis by Au Nanoparticles: Reforming of Methanol. *Gold Bull.* **2004**, *37*, 170–173. [CrossRef]
220. Speltini, A.; Sturini, M.; Maraschi, F.; Dondi, D.; Fisogni, G.; Annovazzi, E.; Profumo, A.; Buttafava, A. Evaluation of UV-A and solar light photocatalytic hydrogen gas evolution from olive mill wastewater. *Int. J. Hydrogen Energy* **2015**, *40*, 4303–4310. [CrossRef]
221. Caravaca, A.; Jones, W.; Hardacre, C.; Bowker, M. H_2 production by the the photocatalytic reforming of cellulose and rawbiomass using Ni, Pd, Pt and Au on titania. *Proc. R. Soc. A* **2016**, *472*, 20160054. [CrossRef] [PubMed]
222. Chen, W.-T.; Chan, A.; Sun-Waterhouse, D.; Moriga, T.; Idriss, H.; Waterhouse, G.I.N. Ni/TiO_2: A promising low-cost photocatalytic system for solar H_2 production from ethanol–water mixtures. *J. Catal.* **2015**, *316*, 43–53. [CrossRef]
223. Chen, W.-T.; Jovic, V.; Sun-Waterhouse, D.; Idriss, H.; Waterhouse, G.I.N. The role of CuO in promoting photocatalytic hydrogen production over TiO_2. *Int. J. Hydrogen Energy* **2013**, *38*, 15036–15048. [CrossRef]
224. Melián, E.P.; Suárez, M.N.; Jardiel, T.; Rodríguez, J.M.D.; Caballero, A.C.; Araña, J.; Calatayud, D.G.; Díaz, O.G. Influence of nickel in the hydrogen production activity of TiO_2. *Appl. Catal. B* **2014**, *152–153*, 192–201. [CrossRef]
225. Cobo, S.; Heidkamp, J.; Jacques, P.-A.; Fize, J.; Fourmond, V.; Guetaz, L.; Jousselme, B.; Ivanova, V.; Dau, H.; Palacin, S.; et al. A Janus cobalt-based catalytic material for electro-splitting of water. *Nat. Mater.* **2012**, *11*, 802–807. [CrossRef] [PubMed]
226. Fujita, S.-I.; Kawamori, H.; Honda, D.; Yoshida, H.; Arai, M. Photocatalytic hydrogen production from aqueous glycerol solution using NiO/TiO_2 catalysts: Effects of preparation and reaction conditions. *Appl. Catal. B* **2016**, *181*, 818–824. [CrossRef]
227. Su, R.; Tiruvalam, R.; Logsdail, A.J.; He, Q.; Downing, C.A.; Jensen, M.T.; Dimitratos, N.; Kesavan, L.; Wells, P.P.; Bechstein, R.; et al. Designer Titania-Supported Au-Pd Nanoparticles for Efficient Photocatalytic Hydrogen Production. *ACS Nano* **2014**, *8*, 3490–3497. [CrossRef] [PubMed]
228. Gallo, A.; Montini, T.; Marelli, M.; Minguzzi, A.; Gombac, V.; Psaro, R.; Fornasiero, P.; Dal Santo, V. H_2 Production by Renewables Photoreforming on Pt–Au/TiO_2 Catalysts Activated by Reduction. *ChemSusChem* **2012**, *5*, 1800–1811. [CrossRef] [PubMed]
229. Hu, Z.; Yu, J.C. Pt_3Co-loaded CdS and TiO_2 for photocatalytic hydrogen evolution from water. *J. Mater. Chem. A* **2013**, *1*, 12221–12228. [CrossRef]
230. Jung, M.; Hart, J.N.; Boensch, D.; Scott, J.; Ng, Y.H.; Amal, R. Hydrogen evolution via glycerol photoreforming over Cu–Pt nanoalloys on TiO_2. *Appl. Catal. A* **2016**, *518*, 221–230. [CrossRef]
231. Han, B.; Hu, Y.H. MoS_2 as a co-catalyst for photocatalytic hydrogen production from water. *Energy Sci. Eng.* **2016**, *4*, 285–304. [CrossRef]
232. Xiang, Q.; Yu, J.; Jaroniec, M. Synergetic Effect of MoS_2 and Graphene as Cocatalysts for Enhanced Photocatalytic H_2 Production Activity of TiO_2 Nanoparticles. *J. Am. Chem. Soc.* **2012**, *134*, 6575–6578. [CrossRef] [PubMed]

233. Xiang, Q.; Cheng, F.; Lang, D. Hierarchical Layered WS_2/Graphene-Modified CdS Nanorods for Efficient Photocatalytic Hydrogen Evolution. *ChemSusChem* **2016**, *9*, 996–1002. [CrossRef] [PubMed]
234. Mahler, B.; Hoepfner, V.; Liao, K.; Ozin, G.A. Colloidal Synthesis of 1T-WS_2 and 2H-WS_2 Nanosheets: Applications for Photocatalytic Hydrogen Evolution. *J. Am. Chem. Soc.* **2014**, *136*, 14121–14127. [CrossRef] [PubMed]
235. Zong, X.; Yan, H.; Wu, G.; Ma, G.; Wen, F.; Wang, L.; Li, C. Enhancement of Photocatalytic H_2 Evolution on CdS by Loading MoS_2 as Cocatalyst under Visible Light Irradiation. *J. Am. Chem. Soc.* **2008**, *130*, 7176–7177. [CrossRef] [PubMed]
236. Wang, D.; Li, R.; Zhu, J.; Shi, J.; Han, J.; Zong, X.; Li, C. Photocatalytic Water Oxidation on $BiVO_4$ with the Electrocatalyst as an Oxidation Cocatalyst: Essential Relations between Electrocatalyst and Photocatalyst. *J. Phys. Chem. C* **2012**, *116*, 5082–5089. [CrossRef]
237. Lutterman, D.A.; Surendranath, Y.; Nocera, D.G. A Self-Healing Oxygen-Evolving Catalyst. *J. Am. Chem. Soc.* **2009**, *131*, 3838–3839. [CrossRef] [PubMed]
238. Di, T.; Zhu, B.; Zhang, J.; Cheng, B.; Yu, J. Enhanced photocatalytic H_2 production on CdS nanorod using cobalt-phosphate as oxidation cocatalyst. *Appl. Surf. Sci.* **2016**, *389*, 775–782. [CrossRef]
239. Bernareggi, M.; Dozzi, M.V.; Bettini, L.G.; Ferretti, A.M.; Chiarello, G.L.; Selli, E. Flame-Made Cu/TiO_2 and Cu-Pt/TiO_2 Photocatalysts for Hydrogen Production. *Catalysts* **2017**, *7*, 301. [CrossRef]
240. Wu, G.; Chen, T.; Su, W.; Zhou, G.; Zong, X.; Lei, Z.; Li, C. H_2 production with ultra-low CO selectivity via photocatalytic reforming of methanol on Au/TiO_2 catalyst. *Int. J. Hydrogen Energy* **2008**, *33*, 1243–1251. [CrossRef]
241. Villa, K.; Doménech, X.; Malato, S.; Maldonado, M.I.; Peral, J. Heterogeneous photocatalytic hydrogen generation in a solar pilot plant. *Int. J. Hydrogen Energy* **2013**, *38*, 12718–12724. [CrossRef]
242. Shimura, K.; Kato, S.; Yoshida, T.; Itoh, H.; Hattori, T.; Yoshida, H. Photocatalytic Steam Reforming of Methane over Sodium Tantalate. *J. Phys. Chem. C* **2010**, *114*, 3493–3503. [CrossRef]
243. Yoshida, H.; Hirao, K.; Nishimoto, J.-I.; Shimura, K.; Kato, S.; Itoh, H.; Hattori, T. Hydrogen Production from Methane and Water on Platinum Loaded Titanium Oxide Photocatalysts. *J. Phys. Chem. C* **2008**, *112*, 5542–5551. [CrossRef]
244. Chiarello, G.L.; Dozzi, M.V.; Scavini, M.; Grunwaldt, J.-D.; Selli, E. One step flame-made fluorinated Pt/TiO_2 photocatalysts for hydrogen production. *Appl. Catal. A* **2014**, *160–161*, 144–151. [CrossRef]
245. Caravaca, A.; Daly, H.; Smith, M.; Mills, A.; Chansaiac, S.; Hardacre, C. Continuous flow gas phase photoreforming of methanol at elevated reaction temperatures sensitised by Pt/TiO_2. *React. Chem. Eng.* **2016**, *1*, 649–657. [CrossRef]
246. Murcia-López, S.; González-Castaño, M.; Flox, C.; Morante, J.R.; Andreu, T. On the role of Cu, Ag and Pt in active titania for gas-phase ethanol photoreforming. *Mater. Sci. Semicond. Process.* **2018**, *73*, 30–34. [CrossRef]
247. Silva, C.G.; Juárez, R.; Marino, T.; Molinari, R.; García, H. Influence of Excitation Wavelength (UV or Visible Light) on the Photocatalytic Activity of Titania Containing Gold Nanoparticles for the Generation of Hydrogen or Oxygen from Water. *J. Am. Chem. Soc.* **2011**, *133*, 595–602. [CrossRef] [PubMed]
248. Zhang, L.; Mohamed, H.H.; Dillert, R.; Bahnemann, D. Kinetics and mechanisms of charge transfer processes in photocatalytic systems: A review. *J. Photochem. Photobiol. C* **2012**, *13*, 263–276. [CrossRef]
249. Xu, C.; Yang, W.; Ren, Z.; Dai, D.; Guo, Q.; Minton, T.K.; Yang, X. Strong Photon Energy Dependence of the Photocatalytic Dissociation Rate of Methanol on TiO_2(110). *J. Am. Chem. Soc.* **2013**, *135*, 19039–19045. [CrossRef] [PubMed]
250. Carraro, G.; Maccato, C.; Gasparotto, A.; Montini, T.; Turner, S.; Lebedev, O.I.; Gombac, V.; Adami, G.; Van Tendeloo, G.; Barreca, D.; et al. Enhanced Hydrogen Production by Photoreforming of Renewable Oxygenates Through Nanostructured Fe_2O_3 Polymorphs. *Adv. Funct. Mater.* **2014**, *24*, 372–378. [CrossRef]
251. Nuo Peh, C.K.; Gao, M.; Wei Ho, G. Harvesting broadband absorption of the solar spectrum for enhanced photocatalytic H_2 generation. *J. Mater. Chem. A* **2015**, *3*, 19360–19367.
252. Patsoura, A.; Kondarides, D.I.; Verykios, X.E. Photocatalytic degradation of organic pollutants with simultaneous production of hydrogen. *Catal. Today* **2007**, *214*, 94–102. [CrossRef]
253. Shamsul, N.S.; Kamarudin, S.K.; Rahman, N.A.; Kofli, N.T. An overview on the production of bio-methanol as potential renewable energy. *Renew. Sustain. Energy Rev.* **2014**, *33*, 578–588. [CrossRef]
254. Hirano, Y.; Sagata, K.; Kita, Y. Selective transformation of glucose into propylene glycol on Ru/C catalysts combined with ZnO under low hydrogen pressures. *Appl. Catal. A* **2015**, *502*, 1–7. [CrossRef]

255. Zhao, G.; Zheng, M.; Zhang, J.; Wang, A.; Zhang, T. Catalytic Conversion of Concentrated Glucose to Ethylene Glycol with Semicontinuous Reaction System. *Ind. Eng. Chem. Res.* **2013**, *52*, 9566–9572. [CrossRef]
256. Devarapalli, M.; Atiyeh, H.K. A review of conversion processes for bioethanol production with a focus on syngas fermentation. *Biofuel Res. J.* **2015**, *7*, 268–280. [CrossRef]
257. Ciriminna, R.; Della Pina, C.; Rossi, M.; Pagliaro, M. Understanding the Glycerol Market. *Eur. J. Lipid Sci. Technol.* **2014**, *116*, 1432–1439. [CrossRef]
258. Huber, G.W.; Iborra, S.; Corma, A. Synthesis of Transportation Fuels from Biomass: Chemistry, Catalysts, and Engineering. *Chem. Rev.* **2006**, *106*, 4044–4098. [CrossRef] [PubMed]
259. Narkis, N.; Henefeld-Fourrier, S.; Rebhun, M. Volatile organic acids in raw wastewater and in physico-chemical treatment. *Water Res.* **1980**, *14*, 1215–1223. [CrossRef]
260. McKendry, P. Energy production from biomass (part 1): Overview of biomass. *Biores. Technol.* **2002**, *83*, 37–46. [CrossRef]
261. Kondarides, D.I.; Daskalaki, V.M.; Patsoura, A.; Verykios, X.E. Hydrogen Production by Photo-Induced Reforming of Biomass Components and Derivatives at Ambient Conditions. *Catal. Lett.* **2008**, *122*, 26–32. [CrossRef]
262. Speltini, A.; Sturini, M.; Maraschi, F.; Dondi, D.; Serra, A.; Profumo, A.; Buttafava, A.; Albini, A. Swine sewage as sacrificial biomass for photocatalytic hydrogen gas production: Explorative study. *Int. J. Hydrogen Energy* **2014**, *39*, 11433–11440. [CrossRef]
263. López, C.R.; Melián, E.P.; Ortega Méndez, J.A.; Santiago, D.E.; Doña Rodríguez, J.M.; González Díaz, O. Comparative study of alcohols as sacrificial agents in H_2 production by heterogeneous photocatalysis using Pt/TiO_2 catalysts. *J. Photochem. Photobiol. A* **2015**, *312*, 45–54. [CrossRef]
264. Wu, Y.; Lu, G.; Li, S. The Role of Cu(I) Species for Photocatalytic Hydrogen Generation Over CuO_x/TiO_2. *Catal. Lett.* **2009**, *133*, 97–105. [CrossRef]
265. Speltini, A.; Sturini, M.; Dondi, D.; Annovazzi, E.; Maraschi, F.; Caratto, V.; Profumo, A.; Buttafava, A. Sunlight-promoted photocatalytic hydrogen gas evolution from water-suspended cellulose: A systematic stud. *Photochem. Photobiol. Sci.* **2014**, *13*, 1410–1419. [CrossRef] [PubMed]
266. Simon, T.; Bouchonville, N.; Berr, M.J.; Vaneski, A.; Adrović, A.; Volbers, D.; Wyrwich, R.; Döblinger, M.; Susha, A.S.; Rogach, A.L.; et al. Redox shuttle mechanism enhances photocatalytic H_2 generation on Ni-decorated CdS nanorods. *Nat. Mater.* **2014**, *13*, 1013–1018.
267. McCullagh, C.; Skillen, N.; Adams, M.; Robertson, P.K.J. Photocatalytic reactors for environmental remediation: A review. *J. Chem. Technol. Biotechnol.* **2011**, *86*, 1002–1017. [CrossRef]
268. Gupta, R.B. Hydrogen fuel. In *Production, Transport and Storage*; CRC Press, Taylor & Francis Group: Boca Raton, FL, USA, 2009; pp. 39–42, ISBN 978-1-4200-4575-8.
269. Leung, D.Y.C.; Caramanna, G.; Maroto-Valer, M.M. An overview of current status of carbon dioxide capture and storage technologies. *Renew. Sustain. Energy Rev.* **2014**, *39*, 426–443. [CrossRef]